

NONLINEAR FOUR WAVE INTERACTIONS AND FREAK WAVES

Peter A.E.M. Janssen,
E.C.M.W.F.,
Shinfield Park,
Reading, RG2 9AX,
U.K.
23 April 2002

Abstract. Four-wave interactions are shown to play an important role in the evolution of the spectrum of surface gravity waves. This follows from direct simulations of an ensemble of ocean waves using the Zakharov equation. The theory of homogeneous four-wave interactions, extended to include effects of nonresonant transfer, compares favourably with the ensemble averaged results of the Monte Carlo simulations. In particular, there is good agreement regarding spectral shape. Also, the kurtosis of the surface elevation probability distribution is well-determined by theory even for waves with a narrow spectrum and large steepness. These extreme conditions are favourable for the occurrence of freak waves.

1. Introduction

Presently, there is a considerable interest in understanding the occurrence of freak waves. The notion of freak waves was first introduced by Draper (1965), and this term is applied for single waves that are extremely unlikely as judged by the Rayleigh distribution of wave heights (Dean, 1990). In practice, a wave with wave height H (defined as the distance from crest to trough) exceeding the significant wave height H_S by a factor 2.2 is considered to be a freak wave. It is difficult to collect hard evidence on such extreme wave phenomena because they occur so rarely. Nevertheless, observational evidence from time series collected over the past decade does suggest that for large surface elevations the probability distribution for the surface elevation deviates substantially from the one that follows from linear theory with random phase, namely the Gaussian distribution (cf. e.g. Wolfram and Linfoot, 2000).

There are a number of reasons why freak wave phenomena may occur. Often, extreme wave events can be explained by the presence of ocean currents or bottom topography that may cause wave energy to focus in a small area due to refraction, reflection and wave trapping. These mechanisms are well understood and may be explained by linear wave theory (cf. e.g. Lavrenov, 1998).

Trulsen and Dysthe (1997) argue, however, that it is not well understood why exceptionally large waves may occur in the open ocean away from non-uniform currents or bathymetry. As an example they discuss the case of an extreme wave event that happened on January 1, 1995 in the Norwegian sector of the North Sea. Their basic premise is that these waves can be produced by nonlinear self modulation of a slowly varying wave train. An example of nonlinear modulation or focussing is the instability of a uniform narrow-band wave train to side-band perturbations. This instability, known as the side-band, modulational or Benjamin-Feir (1967) instability, will result in focusing of wave energy in space and/or time as is illustrated by the experiments of Lake et al (1977).

To a first approximation the evolution in time of the envelope of a narrow-band wave train is described by the nonlinear Schrödinger equation. This equation, which occurs in many branches of physics, was first discussed in the general context of nonlinear dispersive waves by Benney and Newell (1967). For water waves it was first derived by Zakharov (1968) using a spectral method and by Hasimoto and Ono (1972) and Davey (1972) using multiple-scale methods. The nonlinear Schrödinger equation in one-space dimension may be solved by means of the inverse scattering transform. For vanishing boundary conditions Zakharov and Shabat (1972) found that for large times the solution consists of a combination of envelope solitons and radiation modes, in analogy with the solution of the Korteweg-de Vries equation. However, for two-dimensional propagation, Zakharov and Rubenchik (1974)

discovered that envelope solitons are unstable to transverse perturbations, while Cohen, Watson and West (1976) found that a random wave field would break up envelope solitons. This meant that solitons could not be used as building blocks of the nonlinear evolution of gravity waves.

For periodic boundary conditions the solution of the nonlinear Schrödinger equation is more complex. Linear stability analysis of a uniform wave train shows that close side-bands grow exponentially in time in good qualitative agreement with the experimental results of Benjamin and Feir (1967) and Lake et al (1977). For large times there is a considerable energy transfer from the carrier wave to the side-bands. In one-space dimension, if there is only one unstable side-band, Fermi-Pasta-Ulam recurrence occurs (Yuen and Ferguson, 1978) in qualitative agreement with the experiments of Lake et al (1977). In the presence of many unstable side-bands, the evolution of a narrow band wave train becomes much more complex. No recurrence is then found (Caponi et al, 1982) and these authors have termed this confined chaos in a nonlinear wave system because most of the energy resides in the unstable modes. Also, in two-space dimensions (2D) the phenomenon of recurrence is the exception rather than the rule. In addition, in 2D the instability region is unbounded in the perturbation wave vector space, resulting in energy leakage to high wave number modes, hence there is no confined chaos in 2D (Martin and Yuen, 1980). This suggests that the 2D nonlinear Schrödinger equation is inadequate to describe the evolution of weakly nonlinear waves. This was pointed out already by Longuet-Higgins (1978) who performed a stability analysis on the exact equations and found that the instability region is finite in extent. More realistic evolution equations such as the fourth-order evolution equation of Dysthe (1979) or the Zakharov equation (1968) are needed to give an appropriate description of nonlinear gravity waves in two-space dimensions.

Nevertheless, studies of the properties of the nonlinear Schrödinger equation have been vital in understanding the conditions under which freak waves may occur. This was discussed in detail by Osborne et al (2000). For periodic boundary conditions the one-dimensional nonlinear Schrödinger equation may be solved by the inverse scattering method as well. The role of the solitons is then replaced by unstable modes. In the linear regime, these modes just describe the evolution in time according to the Benjamin-Feir instability, while by means of the inverse scattering transform the fate of the unstable mode may be followed right into the nonlinear regime. Using the inverse scattering transform the solution of the 1D nonlinear Schrödinger equation may be written as a "linear" superposition of stable modes, unstable modes and their mutual nonlinear interactions. Here, the stable modes form a Gaussian background wave field from which the unstable modes occasionally rise up and subsequently disappear again, repeating the process quasi-periodically

in time. Making use of the inverse scattering transform these authors readily construct a few examples of giant waves from the one-dimensional nonlinear Schrödinger equation. The question now is what happens in the case of two-dimensional propagation. The notion of solitons is no longer useful, because solitons are unstable in two-dimensions. Osborne et al (2000) show that unstable modes do indeed still exist and that in the nonlinear regime they can take the form of large amplitude freak waves. Furthermore, the notion of unstable modes seems to be a generic property of deep water wave trains, as the authors find nonlinear unstable modes in both the one and two-dimensional versions of Dysthe's fourth order evolution equation. To summarize this discussion, it seems that freak waves are likely to occur as long as the wave train is subject to nonlinear focussing. In addition, we only need to study the case of one-dimensional propagation, because it captures the essentials of the generation of freak waves.

Therefore, in the context of the deterministic approach to wave evolution there seems to be a reasonable theoretical understanding of why in the open ocean freak waves occur. In ocean wave forecasting practice one follows, however, a stochastic approach, i.e. one attempts to predict the ensemble average of a spectrum of random waves, because knowledge on the phases is not available. The main problem then is to what extent one can make statements regarding the occurrence of freak waves in a random wave field. Of course, in the context of wave forecasting only statements of a probabilistic nature can be made. As freak waves imply considerable deviations from the Normal, Gaussian probability distribution function(pdf) of the surface elevation, the main question therefore is whether we can determine in a reliable manner the pdf of the surface elevation. Since the wave spectrum plays a central role in the stochastic approach the question therefore is whether for given wave spectrum the probability of extreme events may be determined.

Present day wave forecasting systems are based on the energy balance equation (Komen et al, 1994), including a parametrised version of Hasselmann's four-wave nonlinear transfer (Hasselmann, 1962). Resonant four-wave interactions for a random, homogeneous sea play an important role in the evolution of the spectrum of wind waves, because on the one hand they determine the high-frequency part of the spectrum, giving rise to an ω^{-4} tail (Zakharov & Filonenko, 1968), while on the other hand the peak of the spectrum is shifted towards lower frequencies. The homogeneous nonlinear interactions give rise to deviations from the Gaussian pdf for the surface elevation, because the third order nonlinearity generates fourth cumulants of the pdf, while the finite fourth cumulant results in spectral change. An important issue is, however, whether the standard homogeneous theory can properly describe the generation of freak waves, simply because it does not seem to incorporate the Benjamin-Feir instability mechanism (Alber, 1978,

Alber and Saffman, 1978, Crawford et al, 1980, Janssen, 1983b). This follows from simple scaling considerations applied to the Hasselmann evolution equation for four-wave interactions. Since the rate of change of the action density N is proportional to N^3 , the nonlinear transfer occurs on the time scale $T_{NL} = O(1/\epsilon^4\omega_0)$. Here, ϵ is a typical wave steepness, which is assumed to be small, and ω_0 is a typical angular frequency of the wave field. In contrast, the Benjamin-Feir instability occurs on the much faster timescale of $O(1/\epsilon^2\omega_0)$.

The Benjamin-Feir instability is an example of a nonresonant four-wave interaction where the carrier wave is phase-locked with the sidebands. This process cannot be described by a theory that assumes that the Fourier amplitudes are not correlated (i.e. a homogeneous wave field), and in which only resonant four-wave interactions are considered. For an inhomogeneous, Gaussian narrow-band wave train, Alber and Saffman (1978), and Alber (1978) derived an evolution equation for the Wigner distribution of the sea state. Inhomogeneities gave rise to a much faster energy transfer, comparable with the typical time scale of the modulational instability. In fact, these authors discovered the random version of the Benjamin-Feir instability: a random narrow band wave train is unstable to side-band perturbations provided the width of the spectrum is sufficiently narrow. Therefore, one would expect the Alber and Saffman approach to be an ideal starting point for treating freak waves in a random wave context. However, it is emphasized that this approach has its limitations because deviations from Normality have not yet been taken into account. In this paper it will be shown, using numerical simulations of an ensemble of ocean waves, that non-Gaussian effects are quite important while inhomogeneities play only a minor role in the evolution of the ensemble-averaged wave spectrum.

On the other hand, nonresonant interactions appear to be relevant. We extend Hasselmann's treatment of four-wave interactions by including the effects of nonresonant interactions. As a consequence, the resonance function is for short times broader than the usual δ -function and depends on the angular frequency resonance conditions and on time. The standard nonlinear transfer is based on the assumption that the action density spectrum is a slowly varying function of time. It is then argued that the resonance function may be replaced by its large time limit, giving the usual delta function. However, the time span required for the resonance function to evolve towards a delta function is so large that considerable changes in the action density function may have occurred in the mean time. This will be shown for the special case of one dimensional propagation of surface gravity waves. In those circumstances the standard approach to nonlinear wave-wave interactions would not give rise to nonlinear transfer, whereas considerable changes of the wave spectrum occur in the new approach. In fact, there is close agreement between

results on the ensemble averaged spectrum and the kurtosis of the pdf of the surface elevation, as obtained from numerical simulations of an ensemble of ocean waves. Since timeseries from the numerical simulations indicate the occurrence of freak waves when the waves are sufficiently steep (see also Trulsen and Dysthe (1997) or Osborne et al (2000)), the implication is that an approach to nonlinear transfer, that includes nonresonant interactions seems to capture freak wave events. However, it is strongly emphasized that such an approach can only give statements of a probabilistic nature on the occurrence of extreme wave events.

The structure of this paper is as follows. In Section 2 we review developments regarding the evolution of a random wave field, but we discuss only the ideas needed for understanding results in the remainder of this paper. In particular, we extend the standard theory of four wave interactions by including effects of nonresonant interactions and derive an explicit expression for the kurtosis in terms of the action density spectrum. We also discuss Alber and Saffman's key result, that according to lowest order inhomogeneous theory there is only Benjamin-Feir instability when the wave spectrum is sufficiently narrow. In Section 3 we present results from Monte Carlo simulations of the nonlinear Schrödinger equation following similar work by Onorato et al (2000). Only one-dimensional wave propagation is discussed. Apart from reasons of economy (we typically do runs with 500 member ensembles), the main reason for this choice is that for one dimension the nonlinear transfer according to the standard homogeneous theory of four wave interactions vanishes identically. The ensemble averaged evolution of the wave spectrum clearly shows that there is an irreversible energy transfer resulting in a broadening of the spectrum, while the pdf of the surface elevation has considerable deviations from the Gaussian distribution. These deviations from Normality may be described, as expected from four-wave interactions, by means of the fourth cumulant. In case of nonlinear focussing, the correction to the pdf is such that there is an enhanced probability of extreme events, while in the case of nonlinear defocussing (this was achieved by changing the sign of the nonlinear term) the opposite occurs, namely the probability of extreme events is reduced. This is in agreement with results by Tanaka (1991) who found an increase in groupiness in case of nonlinear focussing while in the opposite case of a stable wave train groupiness reduces.

Both the spectral broadening and the fourth cumulant (or kurtosis) are found to depend on a single parameter characterising the narrow-band wave train, namely the ratio of mean square slope to the normalised width of the (frequency) spectrum. It is suggested to call this ratio the Benjamin-Feir Index (BFI). If the BFI is larger than 1 then according to Alber and Saffman (1978) the random wave field is modulationally unstable. This result would suggest that if the BFI is less than 1 no changes in the spectrum occur, while

in the opposite case the unstable side-bands would give rise to a broadening of the wave spectrum. Hence, $BFI = 1$ is a bifurcation point. Our numerical simulations provide no convincing evidence of a bifurcation at $BFI = 1$. Rather, there is already a considerable broadening of the wave spectrum around $BFI = 1$, while the dependence of the broadening on the BFI appears to be smooth rather than abrupt (cf. Tanaka (1991)).

We continue in Section 3 by presenting results from Monte Carlo simulations of the Zakharov equation (Zakharov, 1968). Results are similar in spirit to those obtained with the Nonlinear Schrödinger equation, except that the modulational instability seems to occur for larger BFI. For the nonlinear Schrödinger equation the spectral change owing to nonlinear transfer is symmetrical with respect to the spectral maximum, but this is not the case for Zakharov equation. In the latter case the nonlinear transfer coefficients and the angular frequency are asymmetrical with respect to the spectral peak and as a consequence there is a down-shift of the peak of the spectrum. It is emphasized that this down-shift occurs in the absence of dissipation, while quantities such as action, wave momentum and total wave energy are conserved.

In Section 4 an interpretation of the numerical results of Section 3 is given. Firstly, it is shown that inhomogeneities only play a minor role in the evolution of the wave spectrum, while deviations from Normality are more relevant. Secondly, results from the numerical solution of the extended version of Hasselmann's wave-wave interaction approach are presented and compared with the results from Monte-Carlo simulations. A good agreement is obtained. Apart from the fact that we have given a direct validation of Hasselmann's four-wave theory, it also shows that even in extreme conditions such as occur during the generation of freak waves, reliable estimates of deviations from Normality can be made.

In Section 5 a summary of conclusions is given. Much to our surprise, effects of inhomogeneity only play a minor role in understanding the ensemble averaged evolution of surface gravity waves. Homogeneous four-wave interactions, albeit extended by allowing for a time dependent resonance function, seem to capture most essential features of the averaged nonlinear wave evolution. It seems now possible to estimate the enhanced occurrence of extreme waves and freak waves on the open ocean since the kurtosis may be estimated directly from the wave spectrum.

2. Review of the theory of a random wave field

Our starting point is the Zakharov equation, which is a deterministic evolution equation for surface gravity waves in deep water. It is obtained from the Hamiltonian for water waves, first found by Zakharov (1968). Consider

the potential flow of an ideal fluid of infinite depth. Coordinates are chosen in such a way that the undisturbed surface of the fluid coincides with the x - y plane. The z -axis is pointed upward, and the acceleration of gravity g is pointed in the negative z -direction. Let η be the shape of the surface of the fluid, and let ϕ be the potential of the flow. Hence, the velocity of the flow follows from $\mathbf{u} = -\nabla\phi$.

By choosing as canonical variables

$$\eta, \text{ and, } \psi(\mathbf{x}, t) = \phi(\mathbf{x}, z = \eta, t), \quad (1)$$

Zakharov (1968) showed that the total energy E of the fluid may be used as a Hamiltonian. Here,

$$E = \frac{1}{2} \int \int_{-\infty}^{\eta} dz d\mathbf{x} \left((\nabla\phi)^2 + \left(\frac{\partial\phi}{\partial z}\right)^2 \right) + \frac{g}{2} \int d\mathbf{x} \eta^2. \quad (2)$$

The x -integrals extend over the total basin considered. If an infinite basin is considered the resulting total energy is infinite, unless the wave motion is localized within a finite region. This problem may be avoided by introducing the energy per unit area by dividing (2) by the total surface $L \times L$, where L is the length of the basin, and taking the limit of $L \rightarrow \infty$ afterwards. As a consequence, integrals over wave number \mathbf{k} are replaced by summations while δ -functions are replaced by Kronecker δ 's. For a more complete discussion cf. Komen et al (1994). We will adopt this approach implicitly in the remainder of this paper.

The boundary conditions at the surface, namely the kinematic boundary condition and Bernoulli's equation, are then equivalent to Hamilton's equations,

$$\frac{\partial\eta}{\partial t} = \frac{\delta E}{\delta\psi}, \quad \frac{\partial\psi}{\partial t} = -\frac{\delta E}{\delta\eta}, \quad (3)$$

where $\delta E/\delta\psi$ is the functional derivative of E with respect to ψ , etc. Inside the fluid the potential ϕ satisfies Laplace's equation,

$$\nabla^2\phi + \frac{\partial^2\phi}{\partial z^2} = 0 \quad (4)$$

with boundary conditions

$$\phi(\mathbf{x}, z = \eta) = \psi \quad (5)$$

and

$$\frac{\partial\phi(\mathbf{x}, z)}{\partial z} = 0, \quad z \rightarrow \infty. \quad (6)$$

If one is able to solve the potential problem, then ϕ may be expressed in term of the canonical variables η and ψ . Then the energy E may be evaluated in

terms of the canonical variables, and the evolution in time of η and ψ follows at once from Hamilton's equations (Eq.(3)). This was done by Zakharov (1968), who obtained the deterministic evolution equations for deep water waves by solving the potential problem (4-6) in an iterative fashion for small steepness ϵ . In addition, the Fourier transforms of η and ϕ were introduced, while results could be expressed in a concise way by use of the action variable $A(\mathbf{k}, t)$. For example, in terms of A the surface elevation η becomes

$$\eta = \int_{-\infty}^{\infty} d\mathbf{k} \left(\frac{k}{2\omega} \right)^{1/2} [A(\mathbf{k}) + A^*(-\mathbf{k})] e^{i\mathbf{k}\cdot\mathbf{x}}. \quad (7)$$

Here, \mathbf{k} is the wave number vector, k its absolute value, and $\omega = \sqrt{gk}$ denotes the dispersion relation of deep-water, gravity waves. Substitution of the series solution for ϕ into the Hamiltonian (2) gives an expansion of the total energy E of the fluid in terms of wave steepness,

$$E = \epsilon^2 E_2 + \epsilon^3 E_3 + \epsilon^4 E_4 + O(\epsilon^5). \quad (8)$$

Retaining only the second-order term of E corresponds to the linear theory of surface gravity waves, the third-order term corresponds to three-wave interactions, and the fourth-order term corresponds to four-wave interactions. Since resonant three-wave interactions are absent for deep-water gravity waves, a meaningful description of the wave field is only obtained by going to fourth order in ϵ . In fact, Krasitskii (1990) has shown that in the absence of resonant three wave interactions there is a nonsingular, canonical transformation from the action variable A to the new variable a that allows elimination of the third order contribution to the wave energy. Loosely speaking, the new variable a describes the free wave part of the wave field. Apart from a constant factor, the energy of the free waves becomes,

$$E = \int d\mathbf{k}_1 \omega_1 a_1^* a_1 + \frac{1}{2} \int d\mathbf{k}_{1,2,3,4} T_{1,2,3,4} a_1^* a_2^* a_3 a_4 \delta_{1+2-3-4}, \quad (9)$$

where $a_1 = a(\mathbf{k}_1)$, etc., δ is the Dirac delta function and the interaction matrix T is given by Krasitskii (1990). The interaction matrix enjoys a number of symmetry conditions, of which the most important one is $T_{1,2,3,4} = T_{3,4,1,2}$ as this condition implies that E is conserved. Hamilton's equations now become the single equation

$$i \frac{\partial a}{\partial t} = \frac{\delta E}{\delta a^*}, \quad (10)$$

and, evaluating the functional derivative of E with respect to a^* , the evolution equation for a becomes

$$\frac{\partial a_1}{\partial t} + i\omega_1 a_1 = -i \int d\mathbf{k}_{2,3,4} T_{1,2,3,4} a_2^* a_3 a_4 \delta_{1+2-3-4}, \quad (11)$$

known as the Zakharov equation. Apart from the free wave energy (9) the Zakharov equation admits conservation of action and of wave momentum as

$$\begin{aligned} a) \quad & \frac{d}{dt} \int d\mathbf{k}_1 a_1 a_1^* = 0, \\ b) \quad & \frac{d}{dt} \int d\mathbf{k}_1 \mathbf{k}_1 a_1 a_1^* = 0. \end{aligned} \tag{12}$$

2.1. COMMENTS ON THE ZAKHAROV EQUATION

The properties of the Zakharov equation have been studied in great detail by, for example, Crawford et al (1981) (for an overview see Yuen and Lake, 1982). Thus the nonlinear dispersion relation, first obtained by Stokes (1947), follows from Eq.(11), while also the instability of a weakly nonlinear, uniform wave train (the so-called Benjamin-Feir instability) is well described by the Zakharov equation; the results on growth rates, for example, are qualitatively in good agreement with the results of Longuet-Higgins (1978). However, these results were obtained with a form of the interaction matrix T that did not result in a Hamiltonian form of Eq.(11). Krasitskii (1990) found the correct canonical transformation to eliminate the cubic interactions, which resulted in a T that satisfied the appropriate symmetry conditions for Eq.(11) to be Hamiltonian. Krasitskii and Kalmykov (1993) studied the differences between the Hamiltonian and the non-Hamiltonian forms of the Zakharov equation but only for large amplitude differences in the solution were found.

In this paper we initially use a narrow-band approximation to the Zakharov equation, because the main impact of the Benjamin-Feir instability is found near the spectral peak. This approximate evolution equation is obtained by means of a Taylor expansion of angular frequency ω and the interaction matrix T around the carrier wave number \mathbf{k}_0 . The nonlinear Schrödinger equation is then obtained by using only the lowest order approximation to T given by k_0^3 , while angular frequency ω is expanded to second order in the modulation wave number $\mathbf{p} = \mathbf{k} - \mathbf{k}_0$. The main advantage of the use of the nonlinear Schrödinger equation is that many properties of this equation are known and that it can be solved numerically in an efficient way. The drawback is, however, that it overestimates the growth rates of the Benjamin-Feir instability and that the nonlinear energy transfer is symmetrical with respect to the carrier wave number. For this reason, we study solutions of the complete Zakharov equation as well, using the Krasitskii (1990) expression for the interaction matrix T . Similarly, one could study higher-order evolution equations such as the one by Dysthe (1979), but we found that spectra may become so broad that the narrow-band approximation becomes invalid.

Another reason for studying the nonlinear Schrödinger equation is that it allows us to introduce an important parameter which will be used to stratify

the numerical and theoretical results. From the physical point of view we are basically studying a problem that concerns the balance between dispersion of the waves and its nonlinearity. For the full Zakharov equation it will be difficult to introduce a unique measure of, for example, nonlinearity because the nonlinear transfer matrix T is a complicated function of wave number. However, in the narrow-band approximation, giving the nonlinear Schrödinger equation, this is more straight-forward to do. Balancing the nonlinear term and the dispersive term in the narrow-band version of Eq.(11) therefore gives the dimensionless number

$$-\frac{gT_0}{\omega_0} \frac{1}{k_0^4 \omega_0''} \frac{s^2}{\sigma_\omega'^2}. \quad (13)$$

Since our interest is in the dynamics of a continuous spectrum of waves the slope parameter s and the relative width σ_ω' of the frequency spectrum relate to spectral properties, hence $s = (k_0^2 \langle \eta^2 \rangle)^{\frac{1}{2}}$, with $\langle \eta^2 \rangle$ the average surface elevation variance, and $\sigma_\omega' = \sigma_\omega / \omega_0$. For positive sign of the dimensionless parameter (13) there is focussing (modulational instability) while in the opposite case there is defocussing of the weakly nonlinear wave train. Based on this we introduce the Benjamin-Feir(BF) Index, which, apart from a constant, is the square root of the dimensionless number (13). Using the dispersion relation for deep-water gravity waves and the expression for the nonlinear interaction coefficient, $T_0 = k_0^3$, the BF Index becomes,

$$BFI = s\sqrt{2}/\sigma_\omega'. \quad (14)$$

The BF Index turns out to be very useful in ordering the theoretical and numerical results presented in the following Sections. For simple initial wave spectra that only depend on the variance and on the spectral width, it can be shown that for the nonlinear Schrödinger equation the solution is completely characterized by the BF Index. For the Zakharov equation this is not the case, but the BF Index is still expected to be a useful parameter for narrow-band wave trains.

2.2. STOCHASTIC APPROACH

The Zakharov equation (11) predicts amplitude and phase of the waves. For practical applications such as wave prediction, the detailed information regarding the phase of the waves is not available. Therefore, at best one can hope to predict average quantities such as the second moment

$$B_{1,2} = \langle a_1 a_2^* \rangle, \quad (15)$$

where the angle brackets denote an ensemble average. Here, we briefly sketch the derivation of the evolution equation for the second moment from the Zakharov equation, assuming a zero mean value, $\langle a_1 \rangle = 0$. It is known,

however, that because of nonlinearity, the evolution of the second moment is determined by the fourth moment, and so on, resulting in an infinite hierarchy of equations (Davidson, 1972). To obtain a meaningful truncation of this hierarchy, it is customary to assume that the probability distribution for a_1 is close to a Gaussian distribution, an assumption which is a reasonable one for small wave steepness ϵ . In that event, higher-order moments can be expressed in lower-order moments. In general, for a zero-mean stochastic variable a_1 , one finds that the fourth moment becomes

$$\langle a_j a_k a_l^* a_m^* \rangle = B_{j,l} B_{k,m} + B_{j,m} B_{k,l} + D_{j,k,l,m}, \quad (16)$$

where D is the so-called fourth cumulant, which vanishes for a Gaussian sea state. Resonant nonlinear interactions, however, will tend to create correlations in such a way that a finite fourth cumulant results. But for small steepness D is expected to be small, so that an approximate closure of the infinite hierarchy of equations may be achieved.

Let us now sketch the derivation of the evolution equation for the second moment $\langle a_i a_j^* \rangle$ from the Zakharov equation (11). To that end, we multiply Eq.(11) for a_i by a_j^* , add the complex conjugate with i and j interchanged, and take the ensemble average:

$$\left[\frac{\partial}{\partial t} + i(\omega_i - \omega_j) \right] B_{i,j} = -i \int d\mathbf{k}_{2,3,4} [T_{i,2,3,4} \langle a_j^* a_2^* a_3 a_4 \rangle \delta_{i+2-3-4} - c.c.(i \leftrightarrow j)], \quad (17)$$

where $c.c.$ denotes complex conjugate, and $i \leftrightarrow j$ denotes the operation of interchanging indices i and j in the previous term. Because of nonlinearity the equation for the second moment involves the fourth moment. Similarly, the equation for the fourth moment involves the sixth moment. It becomes

$$\left[\frac{\partial}{\partial t} + i(\omega_i + \omega_j - \omega_k - \omega_l) \right] \langle a_i a_j a_k^* a_l^* \rangle = -i \int d\mathbf{k}_{2,3,4} [T_{i,2,3,4} \langle a_2^* a_k^* a_l^* a_3 a_4 a_j \rangle \delta_{i+2-3-4} + (i \leftrightarrow j)] + i \int d\mathbf{k}_{2,3,4} [T_{k,2,3,4} \langle a_3^* a_4^* a_l^* a_2 a_i a_j \rangle \delta_{k+2-3-4} + (k \leftrightarrow l)]. \quad (18)$$

So far, no approximations have been made. In the next Section, we discuss the implications of the assumptions of a homogeneous weakly nonlinear wave field. Homogeneity of the wave field, however, does not allow a description of the Benjamin-Feir instability, and therefore in the following Section we discuss the consequences for spectral evolution when the wave field is allowed to be inhomogeneous.

2.3. EVOLUTION OF A HOMOGENEOUS RANDOM WAVE FIELD

A wave field is considered to be homogeneous if the two point correlation function $\langle \eta(\mathbf{x}_1)\eta(\mathbf{x}_2) \rangle$ depends only on the distance $\mathbf{x}_1 - \mathbf{x}_2$. Using the expression for the surface elevation, Eq.(7), it is then straightforward to verify that a wave field is homogeneous provided that the second moment $B_{i,j}$ satisfies

$$B_{i,j} = N_i \delta(\mathbf{k}_i - \mathbf{k}_j), \quad (19)$$

where N_i is the spectral action density, which is equivalent to a number density because $\omega_i N_i$ is the spectral energy density, while $\mathbf{k}_i N_i$ is the spectral momentum density (apart from a factor ρ_w).

For weakly nonlinear waves the fourth cumulant D is small compared to the product of second-order cumulants (this may be verified afterwards, it follows immediately from Eq.(18). Now, invoking the random-phase approximation (i.e. Eq.(16)) with $D = 0$ on Eq.(17), combined with the assumption of a homogeneous wave field results in constancy of the second moment $B_{i,j}$. Hence, the need to go to higher order; that is the fourth moment has to be determined through Eq.(18).

Application of the random phase approximation to the sixth moment and solving Eq.(18) for the fourth cumulant D , subject to the initial value $D(t = 0) = 0$, gives

$$D_{i,j,k,l} = 2T_{i,j,k,l} \delta_{i+j-k-l} G(\Delta\omega, t) [N_i N_j (N_k + N_l) - (N_i + N_j) N_k N_l] \quad (20)$$

where $\Delta\omega$ is short hand for $\omega_i + \omega_j - \omega_k - \omega_l$, and we have made extensive use of the symmetry properties of the nonlinear transfer matrix T , in particular the Hamiltonian symmetry. In addition, we used the property that, according to Eq.(17) the action density N only evolves on the slow time scale. The function G is defined as

$$G(\Delta\omega, t) = i \int_0^t d\tau e^{i\Delta\omega(\tau-t)} = R_r(\Delta\omega, t) + iR_i(\Delta\omega, t), \quad (21)$$

where

$$R_r(\Delta\omega, t) = \frac{1 - \cos(\Delta\omega t)}{\Delta\omega}, \quad (22)$$

while

$$R_i(\Delta\omega, t) = \frac{\sin(\Delta\omega t)}{\Delta\omega}. \quad (23)$$

The function G develops for large time t into the usual generalised functions $P/\Delta\omega$, and $\delta(\Delta\omega)$, since,

$$\lim_{t \rightarrow \infty} G(\Delta\omega, t) = \frac{P}{\Delta\omega} + \pi i \delta(\Delta\omega), \quad (24)$$

a relation which is, strictly speaking, only meaningful inside integrals over wave number when multiplied by a smooth function.

Substitution of Eq.(20) into Eq.(17) eventually results in the following evolution equation for four-wave interactions,

$$\begin{aligned} \frac{\partial}{\partial t} N_4 &= 4 \int d\mathbf{k}_{1,2,3} T_{1,2,3,4}^2 \delta(\mathbf{k}_1 + \mathbf{k}_2 - \mathbf{k}_3 - \mathbf{k}_4) R_i(\Delta\omega, t) \\ &\quad \times [N_1 N_2 (N_3 + N_4) - N_3 N_4 (N_1 + N_2)], \end{aligned} \quad (25)$$

where now $\Delta\omega = \omega_1 + \omega_2 - \omega_3 - \omega_4$. This evolution equation is usually called the Boltzmann equation.

Two limits of the resonance function $R_i(\Delta\omega, t)$ are of interest to mention. For small times we have

$$\lim_{t \rightarrow 0} R_i(\Delta\omega, t) = t \quad (26)$$

while for large times we have

$$\lim_{t \rightarrow \infty} R_i(\Delta\omega, t) = \pi \delta(\Delta\omega). \quad (27)$$

Hence, according to Eq.(25), for short times the evolution of the action density N is caused by both resonant and nonresonant four-wave interactions, while for large times, when the resonance functions evolves towards a δ -function, only resonant interactions contribute to spectral change.

In the standard treatment of resonant wave wave interactions (cf., for example Hasselmann (1962) and Davidson (1972)) it is argued that the resonance function $R_i(\Delta\omega, t)$ may be replaced by its time-asymptotic value (Eq.(27)), because the action density spectrum is a slowly varying function of time. However, the time required for the resonance function to evolve towards a delta function may be so large that in the mean time considerable changes in the action density may have occurred. For this reason we will keep the full expression for the resonance function.

An important consequence of this choice concerns the estimation of a typical time scale T_{NL} for the nonlinear wave-wave interactions in a homogeneous wave field. With ϵ a typical wave steepness and ω_0 a typical angular frequency of the wave field, one finds from the Boltzmann equation(25) that for short times $T_{NL} = O(1/\epsilon^2\omega_0)$, while for large times $T_{NL} = O(1/\epsilon^4\omega_0)$. Hence, although the standard nonlinear transfer, which uses as resonance function Eq.(27), does not capture the physics of the modulational instability (which operates on the fast time scale $1/\epsilon^2\omega_0$), the full resonance function does not suffer from this defect.

It is also important to note that according to the standard theory there is only nonlinear transfer for two-dimensional wave propagation. In the one-dimensional case there is no nonlinear transfer in a homogeneous wave field.

The reason for this is that only those waves interact nonlinearly that satisfy the resonance conditions $\mathbf{k}_1 + \mathbf{k}_2 = \mathbf{k}_3 + \mathbf{k}_4$ and $\omega_1 + \omega_2 = \omega_3 + \omega_4$. In one dimension these resonance conditions can only be met for the combinations $\mathbf{k}_1 = \mathbf{k}_3, \mathbf{k}_2 = \mathbf{k}_4$ or $\mathbf{k}_1 = \mathbf{k}_4, \mathbf{k}_2 = \mathbf{k}_3$. Then, the rate of change of the action density, as given by Eqns.(25 and 27), vanishes identically because of the symmetry properties of the term involving the action densities. This contrasts with the Benjamin-Feir instability which has its largest growth rates for waves in one dimension. On the other hand, using the complete expression for the resonance function, there is always an irreversible nonlinear transfer even in the case of one-dimensional propagation.

The Boltzmann equation, Eq.(25), admits just as the deterministic Zakharov equation, conservation of total action, wave momentum, while the ensemble average of the Hamiltonian (Eq. (9)) is conserved as well (The last conservation law follows from Eqs.(25) by consistently utilizing the assumption of a slowly varying action density). It is emphasized that the Hamiltonian consists of two parts, the energy according to linear wave theory and a nonlinear interaction term. Therefore, unlike the standard theory of four-wave interactions, the linear expression for the wave energy is not conserved. The exception occurs for large times when the resonance function R_i has evolved towards a δ -function, and then just as in the standard theory the linear wave energy is conserved. This follows also from the numerical simulations presented in Section 3 which show that the ensemble average of the Hamiltonian is conserved but, in particular for short times, not the linear wave energy. Furthermore, it should be mentioned that the Boltzmann equation (25) has the time reversal symmetry of the original Zakharov equation, since the resonance function changes sign when time t changes sign. Also, as R_i vanishes for $t = 0$, the time derivative of the action density spectrum is continuous around $t = 0$ and does not show a cusp. (cf. Komen et al, 1994). Nevertheless, despite the fact that there is time reversal, Eq.(25) has the irreversibility property: the memory of the initial conditions gets lost in the course of time owing to phase mixing.

The standard nonlinear transfer in a homogeneous wave field has been studied extensively in the past four decades. The JONSWAP study (Hasselmann et al, 1973) has shown the prominent role played by four-wave interactions in shaping the wave spectrum, and in shifting the peak of the spectrum towards lower frequencies. Modern wave forecasting systems therefore use a parametrization of the nonlinear transfer (Komen et al, 1994).

Our main interest in this paper is in the statistical aspects of random, weakly nonlinear waves in the context of the Zakharov equation. In particular we are interested in the relation between the deviations from the Gaussian distribution and four-wave interactions. Because of the symmetries of the Zakharov equation, the first moment of interest is then the fourth moment

and the related kurtosis. The third moment and its related skewness vanishes: information on the odd moments can only be obtained by making explicit use of Krasitskii's (1990) canonical transformation. Now, the fourth moment $\langle \eta^4 \rangle$ may be obtained in a straightforward manner from Eq.(16) and the expression for the fourth cumulant Eq.(20) as

$$\langle \eta^4 \rangle = \frac{3}{4g^2} \int d\mathbf{k}_{1,2,3,4} (\omega_1 \omega_2 \omega_3 \omega_4)^{\frac{1}{2}} \langle a_1 a_2 a_3^* a_4^* \rangle + c.c \quad (28)$$

Denoting the second moment $\langle \eta^2 \rangle$ by m_0 , deviations from Normality are then most conveniently established by calculating the kurtosis

$$C_4 = \langle \eta^4 \rangle / 3m_0^2 - 1,$$

since for a Gaussian pdf C_4 vanishes. The result for C_4 is

$$C_4 = \frac{4}{g^2 m_0^2} \int d\mathbf{k}_{1,2,3,4} T_{1,2,3,4} \delta_{1+2-3-4} (\omega_1 \omega_2 \omega_3 \omega_4)^{\frac{1}{2}} \\ \times R_r(\Delta\omega, t) N_1 N_2 N_3, \quad (29)$$

where R_r is defined by Eq.(22). For large times, unlike the evolution of the action density, the kurtosis does not involve a Dirac δ -function but rather depends on $P/\Delta\omega$. Therefore, the kurtosis is determined by the resonant and nonresonant interactions. It is instructive to apply Eq.(29) to the case of a narrow band wave spectrum in one dimension. Hence, performing the usual Taylor expansions around the carrier wave number k_0 to lowest significant order, one finds for large times

$$C_4 = \frac{8\omega_0^2 T_0}{g^2 m_0^2 \omega_0''} \int dp_{1,2,3,4} \frac{\delta_{1+2-3-4}}{p_1^2 + p_2^2 - p_3^2 - p_4^2} N_1 N_2 N_3, \quad (30)$$

where $p = k - k_0$ is the wave number with respect to the carrier. It is seen that the sign of the kurtosis is determined by the ratio T_0/ω_0'' , which is the same parameter that determines whether a wave train is stable or not to side-band perturbations. Remark that numerically the integral is found to be negative, at least for bell-shaped spectra. Hence, from Eq.(30) it is immediately plausible that for an unstable wave system which has negative T_0/ω_0'' the kurtosis will be positive and thus will result in an increased probability of extreme events. On the other hand for a stable wave system there will be a reduction in the probability of extreme events.

Finally, a further simplification of the expression for the kurtosis may be achieved if it is assumed that the wave number spectrum $F(p) = \omega_0 N(p)/g$ only depends on two parameters namely, the variance m_0 and the spectral width σ_k . Introduce the scaled wave number $x = p/\sigma_k$ and the correspondingly scaled spectrum $m_0 H(x) dx = F(p) dp$. Then, using the deep-water dispersion relation and $T_0 = k_0^3$, Eq.(30) becomes

$$C_4 = -8 \left(\frac{s}{\sigma'_\omega} \right)^2 J, \quad (31)$$

where s is the significant steepness $k_0 m_0^{\frac{1}{2}}$ while σ'_ω is the relative width in angular frequency space $\sigma_\omega/\omega_0 = 0.5\sigma_k/k_0$. The parameter J is given by the expression

$$J = \int dx_{1,2,3,4} \frac{\delta_{1+2-3-4}}{x_1^2 + x_2^2 - x_3^2 - x_4^2} H_1 H_2 H_3,$$

and is independent of the spectral parameters m_0 and σ_k . Therefore, Eq.(31) suggests a simple dependence of the kurtosis on spectral parameters. In fact, the kurtosis depends on the square of the BF index introduced in Eq.(13).

2.4. EVOLUTION OF AN INHOMOGENEOUS RANDOM WAVE FIELD

The Benjamin-Feir instability is the result of a nonlinear interaction of waves that are phase-locked, as the carrier wave is phase-locked with the sidebands and therefore this process cannot be described by a theory that assumes that the Fourier amplitudes are not correlated, as expressed by the assumption of homogeneity of the wave field (cf. Eq.(19)). Therefore, this suggests that local nonlinear events such as freak waves could be beyond the scope of the standard description of ocean waves.

The investigation of the effect of inhomogeneities on the nonlinear energy transfer started with the work of Alber (1978), and Alber and Saffman (1978), while Crawford et al (1980) combined the effects of inhomogeneity and non-Normality on the evolution of weakly nonlinear water waves. A review of this may be found in Yuen and Lake (1982). We will only discuss the lowest order effects of inhomogeneity, disregarding any effects resulting from deviations from Normality, and we only discuss one-dimensional wave propagation.

Hence, we do not impose the condition of a homogeneous wave field (cf. Eq.(19)). Now invoking the Gaussian approximation on the fourth moment (16 with $D = 0$) and substituting the result in the evolution equation for the second moment, Eq.(17), gives

$$\left[\frac{\partial}{\partial t} + i(\omega_i - \omega_j) \right] B_{i,j} = -2i \int d\mathbf{k}_{2,3,4} [T_{i,2,3,4} \delta_{i+2-3-4} B_{3,j} B_{4,2} - T_{j,2,3,4} \delta_{j+2-3-4} B_{i,3} B_{2,4}] \quad (32)$$

Here, we used the property that the second moment B is hermitian, $B_{i,j} = B_{j,i}^*$, and we made use of the symmetry properties of T .

In principle, Eq.(32) could be used to study the (in)stability of a homogeneous wave spectra, but to our knowledge this has not been done so far. In stead of this, Alber (1978) and Alber and Saffman (1978) studied the stability of a narrow-band, homogeneous wave spectrum. Following Crawford et al (1980) and Yuen and Lake (1982), a considerable simplification of the evolution equation for $B_{i,j}$ may be achieved by expanding angular frequency

ω and interaction coefficient T around the carrier wave number k_0 . At the same time one introduces the sum and difference wave numbers

$$n = \frac{1}{2}(k_i + k_j), m = k_i - k_j \quad (33)$$

while we introduce the relative wave number $p = n - k_0$. The correlation function B is from now on regarded as a function m and n . Realising that in the narrow band approximation n is close to k_0 while m is small, one obtains from Eq.(32) the following approximate evolution equation for B ,

$$\left[\frac{\partial}{\partial t} + im(\omega'_0 + p\omega''_0) \right] B_{n,m} = -2iT_0 \int dl [B_{n-\frac{1}{2}l, m-l} - B_{n+\frac{1}{2}l, m-l}] \int dk B_{k,l}. \quad (34)$$

Here, a prime denotes differentiation with respect to the carrier wave number k_0 , while $T_0 = k_0^3$. A key role in the work of Alber and Saffman is played by the envelope spectral function $W(p, x, t)$, which is in fact a Wigner distribution (Wigner, 1932). It is related to the Fourier transform of $B(n, m, t)$ with respect to m ,

$$W(p, x, t) = \frac{2\omega_0}{g} \int dm e^{imx} B(n, m, t). \quad (35)$$

and a homogeneous sea state simply has a Wigner distribution which is independent of the spatial coordinate x , in agreement with the definition of homogeneous sea given in Eq.(19). In terms of the Wigner distribution Eq.(34) becomes a transport equation in x, p and t , which bears a similarity with the Vlasov Equation from plasma physics. This transport equation is obtained by means of a Taylor expansion of the difference term in the right-hand side of (34) with respect to l , giving an infinite sum. The result is

$$\left[\frac{\partial}{\partial t} + (\omega'_0 + p\omega''_0) \frac{\partial}{\partial x} \right] W = \frac{gT_0}{\omega_0} \frac{\partial \rho}{\partial x} \frac{\partial W}{\partial p} + \dots, \quad (36)$$

where $\rho(x, t) = 2 \langle \eta^2 \rangle$ is the mean square envelope variance, given by

$$\rho(x, t) = \int dp W(p, x, t), \quad (37)$$

while the dots on the right-hand side of Eq.(36) represent the remaining terms of the Taylor series expansion. Note that all terms of the series are required to properly recover the random-version of the Benjamin-Feir instability.

Alber and Saffman (1978) and Alber (1978) studied the stability of a homogeneous spectrum and found that it is unstable to long wave length perturbations if the width of the spectrum is sufficiently small. In other words,

in case of instability inhomogeneities would be generated by what we term the random version of the Benjamin-Feir instability, therefore violating the assumption of homogeneity made in the standard theory of wave-wave interactions.

To see whether a homogeneous spectrum $W_0(p)$ is stable or not, one proceeds in the usual fashion by perturbing $W_0(p)$ slightly according to

$$W = W_0(p) + W_1(p, x, t), W_1 \ll W_0. \quad (38)$$

Linearizing the evolution equation for W around the equilibrium W_0 and considering normal mode perturbations one obtains a dispersion relation between the angular frequency ω and the wave number k of the perturbation. Instability is found for $Im(\omega) > 0$. Alber (1978) considered as special case the Gaussian spectrum

$$W_0(p) = \frac{\langle a_0^2 \rangle}{\sigma_k \sqrt{2\pi}} \exp\left(-\frac{p^2}{2\sigma_k^2}\right), \quad (39)$$

where $\langle a_0^2 \rangle$ is a constant envelope variance and σ_k is the width of the spectrum in wave number space. Stability of the random wave train was found when the relative width of the spectrum, σ_k/k_0 , exceeds a measure of mean square slope. In terms of the relative width σ_ω/ω_0 of the frequency spectrum, which is just half the relative width for the wave number spectrum, one finds stability if

$$\frac{\sigma_\omega}{\omega_0} > (k_0^2 \langle a_0^2 \rangle)^{\frac{1}{2}}, \quad (40)$$

while in the opposite case there is instability of the random wave train. Note that in terms of the BF Index the stability condition Eq.(40) simply becomes $BFI < 1$.

As a consequence, one should expect to find in nature spectra with a width larger than the right hand side of Eq.(40), because for smaller width the random version of the Benjamin-Feir instability would occur, resulting in a rapid broadening of the spectral shape. For a random narrow-band wave train this broadening is an irreversible process because of phase mixing (Janssen, 1983b). The broadening of the spectrum is associated with the generation of inhomogeneities in the wave field. To appreciate this point, we mention that the evolution equation (36) satisfies a number of conservation laws. Using the already introduced envelope surface elevation variance $\rho(x)$ the first few conservation laws are given by

$$\begin{aligned} a) \quad & \frac{d}{dt} \int dx \rho(x) = 0, \\ b) \quad & \frac{d}{dt} \int dx dp pW = 0, \end{aligned} \quad (41)$$

$$c) \frac{d}{dt} \left[\omega_0'' \int dx dp p^2 W + \frac{gT_0}{\omega_0} \int dx \rho^2(x) \right] = 0,$$

assuming periodic boundary conditions in x -space and the vanishing of W for large p . The first equation expresses conservation of wave variance, the second one implies conservation of wave momentum while the last one is the most interesting one in our present discussion because it relates the rate of change of spectral width to the inhomogeneity of the wave field. If the wave field is homogeneous then $\rho(x)$ is independent of x and the second integral in Eq.(41c) is then, because of the first conservation law, independent of time. Therefore, for a homogeneous wavefield there is, as expected, no change in spectral width with time; only inhomogeneities will give rise to spectral change according to lowest order inhomogeneous theory of wave wave interactions.

We remark that the first two conservation laws of (41) may also be obtained immediately from the ensemble average of Eqns.(12), while the last conservation law follows from the expression of the free wave energy given in Eq.(9) by performing ensemble averaging and by invoking the narrow-band approximation. Let us give some of the details of this last derivation. Thus, in the first term the angular frequency is expanded around the carrier wave number \mathbf{k}_0 up to second order, while in the second term the interaction matrix is replaced by its value at \mathbf{k}_0 . For one-dimensional propagation we therefore get,

$$E = \int dp_1 (\omega_0 + p_1 \omega_0' + \frac{1}{2} p_1^2 \omega_0'') a_1 a_1^* + \frac{T_0}{2} \int dp_{1,2,3,4} a_1^* a_2^* a_3 a_4 \delta_{1+2-3-4}.$$

Now, the first two terms are already conserved because of conservation of action and momentum, so we will omit them. Performing ensemble averaging while invoking the assumption of a Gaussian state, i.e. Eq.(16) with $D = 0$, and renaming of the integration variables gives

$$\begin{aligned} \langle E \rangle &= \frac{\omega_0''}{2} \int dp_1 p_1^2 \langle a_1 a_1^* \rangle \\ &+ T_0 \int dp_{1,2,3,4} \langle a_1^* a_3 \rangle \langle a_2^* a_4 \rangle \delta_{1+2-3-4}. \end{aligned}$$

Using the definition for the Wigner distribution, Eq.(35), one then finally arrives at the conservation law (41c).

In order to summarize the present discussion we remark that the central role of the BF Index is immediately evident in the context of the lowest-order inhomogeneous theory of wave-wave interactions. According to the stability criterion (40) there is change of stability for $BFI = 1$. In other words, BFI is a bifurcation parameter: on the short time scale spectra will be stable and therefore do not change if $BFI < 1$ while in the opposite case inhomogeneities will be generated giving rise to a broadening of the spectrum.

However, this prediction follows from an approximate theory that neglects deviations from Normality. In general, considerable deviations from Normality are to be expected, in particular in case of Benjamin-Feir Instability. It is therefore of interest to explore the consequences of non-Normality. This will be done in the next Section by means of a numerical simulation of an ensemble of surface gravity waves.

3. Numerical Simulation of an Ensemble of Waves.

It is important to determine the range of validity of both the homogeneous and inhomogeneous theories of four wave interactions. Both theories assume that the wave steepness is sufficiently small, while the homogeneous theory ignores effects of inhomogeneity, and the inhomogeneous theory assumes that deviations from Normality are small. In order to address these questions we simulate the evolution of an ensemble of waves by running a deterministic model with random initial conditions. Only wave propagation in one dimension will be considered from now on.

For given wave number spectrum $F(k)$, which is related to the action density spectrum through $F = \omega N/g$, initial conditions for the amplitude and phase of the waves are drawn from a Gaussian probability distribution of the surface elevation. The phase of the wave components is then random between 0 and 2π while the amplitude should be drawn from a probability distribution as well (cf. Komen et al, 1994). Regarding each wave component as independent, narrow-band wave trains, a Rayleigh distribution seems to be appropriate for the amplitude. We remark that both phase and amplitude of the waves should be regarded as random variables. Choosing only the phase as random variable would imply that the wave spectrum is known precisely, which is in contrast with observational experience. There is a considerable uncertainty in the wave spectrum as well, which can only be reduced by obtaining frequency spectra from very long time series or wave number spectra from sufficiently large areas. It is straightforward to implement such an approach. However, since the surface elevation is only determined by a finite number of waves, extreme states are not well-represented. As a consequence the kurtosis of the pdf is underestimated. For example, for linear waves it was checked that even with 51 wave components and a wave number resolution of $0.2\sigma_k$ the kurtosis was underestimated by more than 5%. The size of the ensemble was varied between 500 and 5000. On the other hand, drawing random phases but choosing the amplitudes of the waves in a deterministic fashion, as is common practice, gave only an underestimation of kurtosis by 0.1%. Since our main interest is in the proper representation of extreme events, and since computer resources are limited, it was therefore decided to

only take the initial phase as random variable, hence,

$$a(k) = \sqrt{N(k)\Delta k} e^{i\theta(k)}. \quad (42)$$

where $\theta(k)$ is a random phase $= 2\pi x_r$, x_r is a random number between 0 and 1, and Δk the resolution in wave number space.

Each member of the ensemble is integrated for a long enough time to reach equilibrium conditions, typically of the order of 60 dominant wave periods. At every time step of interest the ensemble average of quantities such as the correlation function B , the pdf of the surface elevation and integral parameters such as wave height, spectral width and kurtosis is taken. Typically, the size of the ensemble N_{ens} is 500 members. This choice was made to ensure that quantities such as the wave spectrum were sufficiently smooth and that the statistical scatter in the spectra, which is inversely proportional to $\sqrt{N_{ens}}$, is small enough to give statistically significant results. We now apply this Monte Carlo approach to the nonlinear Schrödinger equation and to the Zakharov equation.

3.1. NONLINEAR TRANSFER ACCORDING TO THE NONLINEAR SCHRÖDINGER EQUATION

As a starting point we choose the Zakharov equation (11) with transfer coefficients and dispersion relation appropriate for the nonlinear Schrödinger equation. The action variable is written as a sum of δ -functions,

$$a(k) = \sum_{i=-N}^{i=N} a_i \delta(k - i\Delta k), \quad (43)$$

where Δk is the resolution in wave number space and $2N + 1$ is the total number of modes. Substitution of Eq.(43) into Eq.(11) gives the following set of ordinary differential equations for the amplitude a_1 ,

$$\frac{d}{dt}a_1 + i\omega_1 a_1 = -i \sum_{1+2-3-4=0} T_{1,2,3,4} a_2^* a_3 a_4 \quad (44)$$

We have solved this set of differential equations with a Runge-Kutta 34 method with variable time step. Relative and absolute error of the solution have been chosen in such a way that conserved quantities such as action, wave momentum and wave energy are conserved to at least five significant digits.

In case of the nonlinear Schrödinger equation we expand the angular frequency around the carrier wave number k_0 up to second order. Again using the difference wave number $p = k - k_0$, we find

$$\omega = \omega_0 + p\omega'_0 + \frac{1}{2}p^2\omega''_0$$

and we eliminate the contribution of the first two terms by transforming to a frame moving with the group velocity. Furthermore, the interaction matrix T is replaced by its value at k_0 . As a result we obtain

$$\frac{d}{dt}a_1 + \frac{i}{2}p_1^2\omega_0''a_1 = -iT_0 \sum_{1+2-3-4=0} a_2^*a_3a_4 \quad (45)$$

where $T_0 = k_0^3$. Amplitude and phase needed for the initial condition for Eq.(45) are generated by Eq.(42) where the wave number spectrum is given by a Gaussian shape,

$$F(p) = \frac{\langle \eta^2 \rangle}{\sigma_k \sqrt{2\pi}} \exp\left(-\frac{p^2}{2\sigma_k^2}\right). \quad (46)$$

Before results on the evolution of the spectral properties of the system (45-46) are presented, we mention that the nonlinear Schrödinger equation admits a straightforward scaling relation. In order to see this, let us remove the dependence of the initial condition on the variance $\langle \eta^2 \rangle$ and the width σ_k by introducing dimensionless variables

$$\begin{aligned} p' &= p/\sigma_k, \\ t' &= (\sigma_k/k_0)^2\omega_0 t, \\ a' &= k_0 a/(s\sqrt{c_0}), \end{aligned} \quad (47)$$

where s is the wave steepness defined below (13) and c_0 is the phase speed corresponding to the carrier wave number, $c_0 = \omega_0/k_0$. Writing the nonlinear Schrödinger equation in terms of these new variables it is immediately evident that for large times its solution can only depend on a single parameter, namely $k_0 s/\sigma_k$, which apart from a constant is just the BF index as defined in Eq.(13).

Initial results obtained from the ensemble average of Monte Carlo Forecasting did not show the simple scaling behaviour with respect to the BF Index, until it was realised that only results should be compared for the same dimensionless time t' , which depends in a sensitive manner on the spectral width σ_k . We therefore integrated the system of equations (45) until a fixed dimensionless time $t' = 15$. A spectral width $\sigma_k = 0.2k_0$ was chosen and without loss of generality the carrier wave number $k_0 = 1$ was taken. The integration interval then corresponds to about 60 wave peak periods. Furthermore, the resolution in wave number space was taken as $\Delta k = \sigma_k/3$ while the total number of wave components was 41, therefore covering a wide range in wave number space. As already noted this choice gave for linear waves a reasonable simulation of the pdf of the surface elevation.

We remark that the specification of a random initial phase has important consequences for the evolution of a narrow-band wave train. This is immediately evident when we compare in Fig. 1 time series for the surface elevation from a run with a fixed initial phase $\theta(k) = 0$ with results from a run with a random choice of the initial phase. While with a deterministic choice of initial phase the nonlinear Schrödinger equation generates in an almost periodic fashion extreme events (Fig. 1a), satisfying the criteria for freak waves, with a random choice of initial phase (Fig. 1b) this is much less evident. Comparing the timeseries from the two cases in detail it is clear that for fixed phase small waves and large waves occur more frequently than in the random phase case. This impression is confirmed by the pdf of the surface elevation shown in Fig. 2. For reference we have also shown the Gaussian probability distribution. In both cases there are considerable deviations from Normality, but in particular for deterministic phase the deviations are large. Similar deviations from the Normal distribution were found by Janssen and Komen (1982). Their approach was entirely analytical and they started from the assumption that for large time the solution of the nonlinear Schrödinger equation would evolve towards a series of envelope solitons, described by an elliptic function. Although they only considered the pdf of the envelope (which under normal conditions is given by the Rayleigh Distribution), one may obtain the pdf of the surface elevation as well. The resulting analytical pdf has similar characteristics as the pdf for the case of deterministic phase.

The Monte Carlo approach was adopted because it is not evident that for the system under discussion the ergodic hypothesis applies. This hypothesis implies replacement of the ensemble average by a time average. However, if one happens to choose initial phases in a way that is favourable for the generation of envelope solitons, then there is a high probability that the solution stays close to the envelope soliton branch and will hardly ever visit other parts of phase space. In order to guarantee a representative picture we therefore decided to perform N_{ens} runs where for each run amplitude and phase are drawn in an independent manner. In the remainder, only ensemble averaged results will be discussed.

In Fig. 3 we show the evolution of the spectral width σ_k with dimensionless time t' for several values of BFI . Here, σ_k is defined using integrals of the wave spectrum F over wave number p :

$$\sigma_k^2 = \frac{\int dp p^2 F(p)}{\int dp F(p)}. \quad (48)$$

We remark that for simulations with the nonlinear Schrödinger equation this turned out to give a remarkable stable estimate of the width of the spectral peak, because the spectra vanish sufficiently rapidly for large p . According to this simulation there is a considerable broadening of the spectrum, which occurs on a fairly short time scale of about 10 peak wave periods. In this

case of one-dimensional propagation the standard theory of nonlinear transfer would give no spectral change. Note that σ_k shows in the early stages of time evolution an overshoot followed by a rapid transition towards an equilibrium value. The number of oscillations around this equilibrium value depend on the precise details of the discretisation scheme. In particular, more, larger amplitude oscillations are found for coarser spectral resolution. The overshoot is in agreement with results of Janssen (1983b), who studied the evolution of a single unstable mode in the context of inhomogeneous theory of wave-wave interactions. For sufficiently narrow spectra, overshoot in the amplitude of the unstable mode was found followed by a damped oscillation towards an equilibrium value. The damping time scale was found to depend on the width of the spectrum, vanishing for small width. Physically, the damping is caused by phase mixing (or destructive interference) and its effect depends on wave number resolution.

As an example of spectral evolution, we show for $BFI = 1.40$ in Fig. 4 initial and final time wave number spectrum. In order to give an idea about the representativeness of the results, 95% confidence limits, based on $N_{ens} - 1$ degrees of freedom, are shown as well. The broadening of the spectrum as caused by the nonlinear interactions seems to be statistically significant. Although the spectral change should be symmetrical with respect to the carrier wave number, i.e $p = 0$, it is clear that there are asymmetries present in the ensemble average of the numerical results. However, these deviations are within the statistical uncertainty. To make sure of this we redid the case for $BFI = 1.40$ but now with an ensemble size of 2000. As expected, statistical uncertainty was reduced by a factor of two while asymmetries were reduced as well.

In order to examine whether the Monte Carlo results show evidence of a bifurcation at $BFI = 1$, we plot in Fig. 5 the relative increase in spectral width, defined as $(\sigma_k(t'_\infty) - \sigma_k(0))/\sigma_k(0)$, as function of the BF index evaluated with the initial value for spectral width. The results suggest that there is only evolution of the spectrum for sufficiently large BF index, but, in contrast to inhomogeneous theory of wave-wave interactions, $BFI = 1$ does not appear to be a bifurcation point, as considerable changes in the wave spectrum already start to occur for $BFI = 1/2$. Although from inhomogeneous theory one would expect a sudden transition from no spectral change to spectral change, Fig. 5 seems to suggest that the transition is gradual. We attribute this discrepancy to the assumption in inhomogeneous theory that deviations from Normality are small, as these may give rise to irreversible changes of the spectrum as well. This will be discussed more extensively in the next Section. It is illuminating to plot the information on spectral width in a slightly different manner, namely by relating the final time value of BFI with its initial value. This is done in Fig. 6 and it clearly shows that for

large times BFI hardly exceeds the value of 1. This seems to agree with the conjecture given in Section 2.2 that according to inhomogeneous theory (c.f. Eq.(40)) one should not expect spectra to have a BFI much larger than 1. According to the Monte Carlo results (cf. Fig. 3) the time scale of change for large BFI is, on average, only a few wave periods.

Nonlinear effects give rise to considerable changes in the probability distribution of the surface elevation from the Gaussian distribution (cf. also Onorato et al, 2000), although the deviations are of course much less than in the cases discussed in Fig. 2. This is shown in Fig. 7 for $BFI = 1.40$. To emphasize the occurrence of extreme events we have plotted the logarithm of the pdf as function of the surface elevation normalised with the wave variance. The Gaussian distribution then corresponds to a parabola. The simulated pdf, in the range of 2-4, shows an almost linear behaviour suggesting an exponential decay of the pdf. Finally, in Fig. 8 we summarize our results on the deviations from Normality by plotting the final time value of the kurtosis $C_4 = \langle \eta^4 \rangle / 3m_0^2 - 1$ as function of the the final time BF Index. Here, the fourth moment $\langle \eta^4 \rangle$ was determined from the pdf of the surface elevation which was obtained by sampling the second half of the time series for the surface elevation at an arbitrarily chosen location. Alternatively, the fourth moment may be obtained from Eq.(28) giving very similar answers. For small nonlinearity one would expect a vanishing kurtosis, but the simulation still underestimates, as already mentioned, the kurtosis by 2%. The kurtosis depends almost quadratically on the Benjamin-Feir Index up to a value close to 1. This quadratic dependence will be explained in the next Section, when an interpretation of results is provided. Near $BFI = 1$, on the other hand, the kurtosis behaves in a more singular fashion, because, in agreement with the discussion of Fig. 6, the Benjamin-Feir Index cannot pass the barrier near 1.

The nonlinear Schrödinger equation(45) for deep water waves is an example where nonlinearity leads to focussing of wave energy and therefore counteracts the dispersion by the linear term which is proportional to ω_0'' . The results from the numerical simulation do indeed suggest that when nonlinearity is sufficiently strong focussing of energy occurs giving considerable enhancements to the probability of extreme events, at least compared to the normal distribution. In the opposite case, when the nonlinear term has opposite sign defocussing of wave energy occurs and one would expect a reduction in the number of extreme events. In order to show this we performed simulations with the nonlinear Schrödinger equation(45) but now with negative nonlinear transfer coefficient ($T_0 = -k_0^3$). Results of this case are shown in the Figs. 5, 6 and 8 while the logarithm of the pdf of the surface elevation is shown in Fig. 9. These plots show that in the case of defocussing the broadening of the spectrum is less dramatic. Furthermore, the final time Benjamin-Feir Index does not have a limiting value of about 1. On the other

hand, the kurtosis for this case is negative, resulting, as can be seen from Fig. 9, in a large reduction of the probability of extreme events. The dependence of the kurtosis on BFI is different from the case of focussing, because there are clear signs of saturation beyond $BFI = 1$, while only in the range $BFI < 0.5$ there is a quadratic dependence of kurtosis C_4 on BFI .

3.2. NONLINEAR TRANSFER ACCORDING TO THE ZAKHAROV EQUATION

The nonlinear Schrödinger equation gives the lowest order effects of finite bandwidth on the evolution of a weakly nonlinear wave train. Dysthe (1979) investigated the consequences of next order in bandwidth and he found a surprisingly large impact on the results for the growth rates of the modulational instability. Similarly, Crawford et al (1981) studied the stability of a uniform wave train using the complete Zakharov equation which retains all the high-order dispersion effects. In general, growth rates are reduced compared to results from the nonlinear Schrödinger equation, therefore according to the Zakharov and the Dysthe equation a uniform wave train is less unstable. In fact, growth rates and thresholds for instability were in better agreement with experimental results of Benjamin & Feir (1967) and Lake et al (1977) (cf. also Janssen, 1983a). The Zakharov and the Dysthe equation have, in addition, the interesting property that the nonlinear transfer coefficient and the angular frequencies are not symmetrical with respect to the carrier wave number. It will be seen that this has important consequences for the spectral shape.

The Dysthe equation follows from the Zakharov equation by expanding angular frequency to third order in the modulation wave number p while the interaction matrix T is expanded up to first order in p . For narrow-band wave trains it gives an accurate description of the sea state. However, wave spectra may become so broad that the narrow-band approximation becomes invalid, and therefore we have chosen to study numerical results from the Zakharov equation.

The Zakharov equation we solved was given by Eq.(44), where the nonlinear transfer coefficient was from Krasitskii (1990), while the exact dispersion relation for deep water gravity waves was taken. The initial condition was provided by Eq.(46). The discretisation details were identical to those of the numerical simulations with the nonlinear Schrödinger equation. Because the Zakharov equation contains all higher-order terms in the modulation wave number p it is not possible to prove that the large time solution of the initial value problem is determined completely by the BF Index, but in good approximation the BF Index can still be used for this purpose as long as the spectra are narrow-banded.

In Fig. 10 we have plotted the ensemble averaged wave number spectrum for $BFI = 1.4$, and it shows a clear down-shift of the peak of the spectrum

while also considerable amounts of energy have been pumped into the high-wave number part of the spectrum. The wave number down-shift is caused by the asymmetries in the nonlinear transfer coefficient and to the same extend by the asymmetries in the angular frequency with respect to the carrier wave number. This was checked by running Eq.(44) with constant nonlinear transfer coefficient, and similarly looking ensemble mean spectra, but with half the wave number down-shift, were obtained. There is also a noticeable broadening of the spectrum. However, because of the increased spectral levels at high wave numbers use of the second moment of the wave number spectrum, as done for the nonlinear Schrödinger equation (cf. (48)), to measure the width of the spectral peak is not appropriate. In stead we use here the width as obtained from fitting the peak of the spectrum with a Gaussian shape-function.

The relation between the final time BFI versus the initial value of BFI is shown in Fig. 11 and is compared with the corresponding one from the nonlinear Schrödinger equation. Also, Fig. 12 shows the normalized kurtosis versus the final time BF index. Results from the Zakharov equation are in qualitative agreement with the ones from the nonlinear Schrödinger equation. However, because growth rates are smaller, the broadening of the spectrum is less, the final time BF index is higher by about 10% and the normalized kurtosis is smaller as well. A unique feature of the Zakharov equation is the down-shift of the peak of the wave number spectrum. This is shown in Fig. 13 where we have plotted the final time value of the peak wave number, normalized with its initial value versus the initial BF index. For large values of BFI reductions in peak wave number of more than 10% are found from the results of the numerical simulations, but the dependence of the down-shift in peak wave number on BFI is not smooth. This is caused by the fact that the ensemble averaged spectra not always have a well-defined spectral peak.

4. Interpretation of numerical results

In the previous Section we have discussed results from the Monte Carlo simulation of the nonlinear Schrödinger equation and the Zakharov equation. These results show that on average there is a rapid broadening of the wave spectrum, while nonlinearity gives rise to considerable deviations from Gaussian statistics. The question now is whether the average of the Monte Carlo results may be obtained in the framework of a simple theoretical description. In Section 2 we have discussed two attempts to achieve this. The first one is the standard theory of wave-wave interactions, extended with the effects of nonresonant four wave interactions. This approach assumes a homogeneous wave field but allows for deviations from the Gaussian sea state. The second theory is the inhomogeneous theory of wave-wave interactions which assumes

that effects of inhomogeneity in the wave field are dominant while deviations from Normality only play a minor role. This approach seems to be an ideal starting point for treating inhomogeneous and nonstationary phenomena such as freak waves because it describes the random version of the Benjamin-Feir instability. Let us therefore first discuss the validity of inhomogeneous theory using results from the Monte Carlo Forecasting of ocean waves obtained from the nonlinear Schrödinger equation.

According to inhomogeneous theory the broadening of the wave spectrum is caused by the inhomogeneity of the wave field. This is clearly expressed by the conservation law (41c) and explained in the discussion that follows. From this conservation law one may therefore obtain a measure of inhomogeneity of the wave field, namely

$$I = \frac{I_2}{I_1^2}, \quad (49)$$

where

$$I_1 = \int dx \rho(x), \quad (50)$$

and

$$I_2 = \int dx \rho^2(x). \quad (51)$$

Here, the integrals over space are weighted by the seize of the domain, and using the definitions for ρ (Eq.37) and the Wigner distribution (cf. Eq.(35)) one may express the inhomogeneity measure I in terms of the correlation function $B(n, m, t)$ as

$$I_1 = \frac{2\omega_0}{g} \sum_p B(p, 0), \quad (52)$$

while

$$I_2 = \left(\frac{2\omega_0}{g} \right)^2 \sum_{p,p',m} B(p, m) B^*(p', m), \quad (53)$$

The correlation functions $B(p, m)$ may be readily obtained from the numerical results for the complex amplitude $a(k, t)$ after ensemble averaging. For a homogeneous wave field $B(p, m) = N(p)\delta(m)$, hence $I_2 = I_1^2$, or $I = 1$.

The initial conditions used in the numerical simulation of waves have been chosen in such a way that the sea state corresponds to a Gaussian one. As a consequence, because the complex amplitudes $a(k, t)$ are not correlated, this implies that initially the sea state is homogeneous as well (cf. Komen et al, 1994). However, the wave ensemble consists of a finite number of members, and this means that the initial probability distribution is not a perfect

Gaussian (the kurtosis is slightly underestimated, for example) but it also means that the initial conditions are slightly inhomogeneous. According to the inhomogeneous theory the perturbations should grow exponentially in time resulting in for example a broadening of the wave spectrum.

For $BFI = 1.4$, the evolution in time of the inhomogeneity I is shown in Fig. 14. Initially, inhomogeneity is small but grows rapidly in the course of time, which is then followed by an oscillation around the level 1.004. This level of inhomogeneity and the variation with time is, however, extremely small (note that for the case of Fig. 1a I is of the order of 3) and it cannot explain the large changes in the wave number spectrum we have seen in the numerical simulations.

In addition, according to the inhomogeneous theory the conservation law (41c) should be satisfied. In Section 3.2 it was explained that this conservation law follows from the conservation of Hamiltonian, assuming that deviations from Normality may be ignored. It is of interest, of course, to test whether it is justified to ignore effects of the fourth cumulant. To that end we compare in Fig. 15 the evolution in time of the Hamiltonian as obtained from the numerical simulation (this will be called the 'exact' Hamiltonian from now on) with the Hamiltonian according to inhomogeneous theory. While the 'exact' Hamiltonian is a constant (at least up to five significant digits), it is clear that the approximate Hamiltonian is not conserved when evaluated using the numerical results. In fact, there are large deviations as the approximate Hamiltonian becomes negative, while the 'exact' Hamiltonian is positive definite. The disagreement between the approximate and the 'exact' Hamiltonian is caused by the neglect of the higher order cumulants. This is immediately clear from Fig. 15 where we have compared the nonlinear contribution to the Hamiltonian according to lowest order inhomogeneous theory (called approximate), with the corresponding nonlinear contribution that includes higher order cumulants (called 'exact'). The approximate nonlinear contribution hardly varies with time, which is in agreement with the results from Fig. 14 that effects of inhomogeneity are small. The 'exact' nonlinear contribution shows a significant variation with time. The difference between 'exact' and approximate are considerable and therefore it is not justified to ignore effects of deviations from Normality in a simple theoretical description of the evolution of the sea state. As a matter of fact, the deviations from Normality are the main reason for the spectral broadening as the time-varying nonlinear contribution to the Hamiltonian, including effects of the fourth order cumulant, just compensates for the changes with time of the linear part of the wave energy. Clearly, according to the Monte Carlo simulations the linear wave energy is not conserved.

In summary, it has been shown that in the inhomogeneous theory of four-wave interactions effects of the generation of the fourth cumulant cannot

be ignored. At the same time we have shown that the numerical ensemble of ocean waves may be regarded to good approximation as a homogeneous ensemble. Hence, the standard theory of four-wave interactions (extended by including nonresonant interactions), which assumes a homogeneous wave field, may be a good candidate to explain the results of the numerical simulations in Section 3.

Therefore, we used the Boltzmann equation(25) to evolve the action density $N(k)$ for the same cases as presented in Section 3. The differential equation was solved with a Runge-Kutta 34 method with variable time step, and the continuous problem was discretized in the same way as was done in case of the solution of the Zakharov equation. Run times using the homogeneous theory are typically two orders of magnitudes faster than when following the ensemble approach.

In contrast to inhomogeneous theory, the standard theory gives a much better approximation to the 'exact' Hamiltonian as shown in Fig. 15. There are, as should be, small differences because the standard theory is an approximation as well, since both effects of inhomogeneity and the sixth cumulant have been neglected. Further results from the discretized version of the homogeneous theory are compared with the ones from the simulations with the nonlinear Schrödinger equation in the Figs. 3-8.

From Fig. 3 which shows the evolution in time of the spectral width for several values of the Benjamin-Feir Index it is seen that for large times there is good agreement between homogeneous theory and the ensemble averaged results from the Monte Carlo simulations. For short times it is however evident that Eq.(25) does not show the overshoot found in the numerical simulations. A likely reason for the absence of overshoot in the theoretical calculations is the assumption that the action density varies slowly compared to the time scale implied by the resonance function $R_i(\Delta\omega, t)$. Both the numerical simulations and homogeneous theory show on the one hand for short times a rapid broadening of the wave spectrum which for large times is followed by a transition towards a steady state. The evolution towards a steady state can be understood as follows: First, it should be noted that, according to Section 2.3, for one-dimensional propagation there is no nonlinear transfer due to resonant nonlinear interactions. Now, initially the resonance function $R_i(\Delta\omega, t)$ will be wide so that nonresonant wave-wave interactions are allowed to modify the action density spectrum. But after about 5-10 wave periods the resonance function becomes progressively narrower until it becomes approximately a δ -function, hence only resonant waves are selected. In that event there is no change of the action density spectrum possible anymore so that for large times a steady state is achieved.

A example of the comparison between theoretical and simulated spectrum is given in Fig. 4. There is a fair agreement between the two. However, it

should be mentioned that typically the simulated spectrum is slightly more peaked than the theoretical one despite the fact that there is a close agreement in spectral width. This agreement in spectral width between theory and simulation is also very much evident in the Figs. 5 and 6 over the full range of the initial value of BFI . In particular note that there is close agreement between the upper limit of the final time BFI from theory and the simulation. Hence, homogeneous theory also provides an explanation of why there is a lower bound to spectral width.

We therefore have the curious situation that both homogeneous and inhomogeneous theory explain why there is a lower bound to spectral width as found in the numerical simulations. However, since it has been shown that inhomogeneities only play a minor role in the numerical simulations it follows that only homogeneous theory provides a proper explanation. In-situ observations from the North Sea seem to indicate the presence of a lower bound to spectral width as well (see for example Janssen, 1991). Although it is impossible to prove at present that at sea inhomogeneities do not play a role, homogeneous theory even seems to give a plausible explanation of the lower bound found at sea.

As discussed in Section 2.3 nonlinearity gives rise to deviations from the normal distribution. We determined the normalised kurtosis using Eq.(29), which is obtained from the fourth cumulant D . Introducing the normalized height $x = \eta/\sqrt{m_0}$, the pdf of the normalized surface elevation x is then given by

$$p(x) = \left(1 + \frac{1}{8} C_4 \frac{d^4}{dx^4} \right) f_0, \quad (54)$$

where f_0 is given by the normal distribution

$$f_0(x) = \frac{1}{\sqrt{2\pi}} \exp\left(-\frac{x^2}{2}\right). \quad (55)$$

Eq.(54) follows from an expansion of the pdf p in terms of orthogonal functions $(d/dx)^n f_0$. Here, n is even because of the symmetry of the Zakharov equation. The expansion coefficients are then obtained by determining the first, second and fourth moment. For the range of BFI studied in this paper it was verified that higher moments only gave a small contribution to the shape of the pdf $p(x)$. The pdf according to theory is compared in Fig. 7 with the simulated one, and a good agreement is obtained, even for extreme sea state conditions. Clearly in the case of nonlinear focussing, the probability of extreme states is, as expected, larger when compared to the normal distribution. Finally, in Fig. 8 theoretical and simulated final time kurtosis is plotted as function of the final time BFI . A good agreement between the two results is obtained even close to the limiting value of the final time BFI .

For $BFI < 1$ both simulated and theoretical kurtosis depend in an almost quadratic fashion on BFI , in agreement with the simple estimates of $C4$ given in Section 2.3 (cf Eq.(31)).

In the case of nonlinear focussing a good agreement between the numerical simulations and the homogeneous theory has been obtained, even for extreme values of the Benjamin-Feir Index. Here, it should be emphasized that at sea BFI has typical values of 0.5 or less and only occasionally values of the order 1 are reached. We have performed simulations to values of BFI of up to 3 and even for these extreme conditions, having large values of kurtosis for example, a reasonable agreement is obtained. This is surprising because the homogeneous theory was derived under the assumption of small deviations from Normality.

In the case of nonlinear defocussing the range of validity of homogeneous theory is much more restricted. This is made plainly clear in the Figs. 5, 6, 8 and 9, where results from the simulations and homogeneous theory are compared for the case of nonlinear defocussing. In order to be able to interpret this comparison we note that homogeneous theory does not distinguish between focussing and defocusing because the nonlinear transfer is independent of the sign of the interaction matrix T . Only the kurtosis depends on the sign of T . Judging from the Figs. 5, 6 and 8 the range of validity of homogeneous theory is restricted to $BFI < 0.6$. In particular, for large BFI there are large qualitative deviations in the kurtosis of the pdf: while from the numerical simulations there are clear signs of saturation in kurtosis, there is no indication of saturation in the results from homogeneous theory. In addition, in case of nonlinear defocussing the kurtosis is negative so that for large normalized elevation x the pdf given in Eq.(54) may become negative. This is clearly unrealistic and in order to correct this undesirable property of homogeneous theory one needs, for large BFI , to take into account the effects of higher than fourth order cumulants as well. It is believed this is the main reason why homogeneous theory has such a restricted validity in this case. In the opposite case of nonlinear focussing the kurtosis is positive, giving for large x a positive correction to the normal distribution. The pdf of the surface elevation is therefore positive, at least for the cases that have been studied here, and as a consequence homogeneous theory has a much larger range of validity.

Finally, we applied homogeneous theory to the Zakharov equation. Results are compared with the numerical simulations in the Figs. 10, 11, 12 and 13. There is a fair agreement between simulated and theoretical spectrum (cf. Fig. 10), between simulated and theoretical final time BFI index (cf. Fig. 11) and normalized kurtosis (cf. Fig. 12). Less favourable is the agreement between simulated and theoretical peak wave number, as show in Fig. 13. The theoretical results show a smooth dependence of wave-number down-

shift on BFI , giving shifts of 20% or more for large values of BFI . However, the simulation shows more scatter while the down-shift is at most 15%. The reason for the scatter in the simulated results is probably that the peak of the wave number spectrum is not always well-defined. In contrast, homogeneous theory gives a smoother spectrum and a well-defined peak of the spectrum.

5. Conclusions

Present day wave forecasting systems are based on a description of the ensemble averaged sea state. In this approach the wave number spectrum plays a central role and its evolution follows from the energy balance equation. The question discussed here is whether it is possible to make statements, necessarily of a statistical nature, on the occurrence of extreme events such as freak waves.

In order to show that this is possible the following approach has been adopted. The starting point is a deterministic set of equations, namely the Zakharov equation or its narrow-band limit the nonlinear Schrödinger equation. There is ample evidence that these equations admit freak wave type solutions. These freak waves occur when the waves are sufficiently steep as nonlinear focussing may then overcome the spreading of energy by linear dispersion. For the same reason the Benjamin-Feir instability occurs. As shown in Fig. 1 the occurrence of freak waves depends in a sensitive manner on the choice of the initial phase of the waves. In addition, on the open ocean waves propagate from different locations towards a certain point of interest, and may therefore be regarded as independent. Hence, for open ocean applications the random phase approximation seems to be appropriate. We therefore simulated the evolution of an ensemble of ocean waves by running a deterministic model with random initial phase. These Monte Carlo simulations are expensive (typically, the size of the ensemble is 500) so that we restrict ourselves to the case of one-dimensional propagation only.

The ensemble average of the results from the Monte Carlo simulations shows that when the Benjamin-Feir Index is sufficiently large (as occurs for the combination of narrow spectra and steep waves) the wave spectrum broadens while at the same time considerable deviations from the Gaussian pdf are found. In case of the Zakharov equation the spectral change is even asymmetrical with respect to the peak of a symmetrical spectrum giving a down-shift of the peak wave number while as a consequence of the conservation of wave action and wave energy considerable amounts of energy are being pumped into the high-wave number part of the spectrum. These spectral changes occur on a short time scale, typically of the order of ten wave periods. This time scale is comparable with the Benjamin-Feir time scale.

The standard homogeneous theory of resonant nonlinear transfer does

not give spectral change in the case of one-dimensional propagation. This theory was therefore extended to allow for nonresonant interactions as well, because the nonlinear focussing related with the Benjamin-Feir Instability is an example of a nonresonant four-wave interaction. This nonlinear four-wave transfer is associated with the generation of higher order cumulants such as the kurtosis. Deviations of the surface elevation pdf from the normal distribution can therefore be expressed in terms of a six-dimensional integral involving the cube of the action spectrum (cf. Eq.(29)). In case of nonlinear focussing there is, for a large range of values of the BFI , a good agreement between the ensemble averaged results from the numerical simulations and homogeneous theory. This is in particular true for the broadening of the spectrum, the spectral shape and the estimation of the kurtosis. Compared to the simulations, theory overestimates, however, the peak wave number down-shift.

Homogeneous theory also explains why for one-dimensional propagation the wave spectrum evolves towards a steady state. The resonance function evolves rapidly towards a δ -function, hence for large times only resonant wave-wave interactions are selected which in one dimension do not give rise to spectral change. This is in sharp contrast with the case of two-dimensional propagation. No trend towards a steady state is expected in that case because resonant four-wave interactions do contribute to a change in the spectrum.

The extended version of the homogeneous four-wave theory has two time scales, a fast one on which the nonresonant interactions take place and a long time scale on which the resonant interactions occur. The nonresonant interactions play a similar role as transients in the solution of an initial value problem. They are simply generated because initially there is a mismatch between the choice of the probability distribution of the waves, a Gaussian, and between the initial choice of the wave spectrum, representing a sea state with narrow-band, steep nonlinear waves. For example, if one could choose a probability distribution function which is in equilibrium with the nonlinear sea state (theoretically one can, by the way), then nonresonant interactions would not contribute. Only resonant wave-wave interactions will then give rise to nonlinear transfer. In the general case for which there is a finite mismatch between pdf and wave spectrum, the nonresonant contribution will die out very quickly owing to phase mixing, but will, nevertheless, as we have seen, result in considerable changes in the wave spectrum. The question therefore is whether there is a need to include effects of nonresonant interactions. This depends on the application. In wave tank experiments, where one can program a wave maker to produce the initial conditions used in this paper, it seems that effects of nonresonant transfer need to be taken account for. For the open ocean case this is not clear. The point is that in nature the combination of steep waves and a strictly Gaussian distribution most likely

does not occur. Changes in nature are expected to be more gradual so that the mismatch between pdf and wave spectrum is small. Only when a wind starts blowing suddenly, hence for short fetches and duration, effects of nonresonant interactions are expected to be relevant. More research in this direction is, however, required.

The results from Monte Carlo Simulations do not provide evidence that there are significant deviations from homogeneity of the ensemble of waves. Deviations from Normality are found to be much more important. Nevertheless, it cannot be concluded from the present study that the inhomogeneous approach of Alber and Saffman (1978) is not relevant for real ocean waves. For example, effects of inhomogeneity might be relevant in fetch-limited, rapidly varying circumstances. However, its effects are expected to be small and therefore only the lowest order approximation, as given explicitly in Eq.(36), needs to be retained.

Finally, for real ocean waves not only four-wave interactions determine the evolution of the wave spectrum. Wind input and dissipation due to white-capping are relevant, and these processes may effect the kurtosis of the sea surface as well. However, it has been shown in this paper that in particular the nonresonant nonlinear transfer acts on a short time scale which is much shorter than the time scales associated with wind input and dissipation source functions used in wave forecasting (Komen et al, 1994). Hence, one would expect that the expression for kurtosis found in this paper (cf Eq.(29)) should be relevant in nature. Nevertheless, nonlinear focussing may result in steep waves. If their steepness exceeds a certain threshold one would expect a significant amount of wave breaking, thus limiting the height of these waves, and effecting the extreme statistics. A realistic, deterministic model of wave breaking is needed to assess the importance of wave breaking in these circumstances. It may be more effective, however, to try to compare results from the present approach directly with observations of extremes collected over a long period.

Acknowledgement The author acknowledges useful and stimulating discussions with Miguel Onorato. His presentation during the 2001 Wise meeting in Canada gave stimulus to have a fresh look at wave-wave interactions and freak waves. Furthermore, the author thanks Theo van Steyn for providing the Runge-Kutta software for accurate integration of a set of ordinary differential equations. Finally, the author thanks Anthony Hollingsworth and Martin Miller for critically reading the manuscript.

6. References

- Alber, I.E., 1978: The effects of Randomness on the Stability of Two-dimensional Surface Wave Trains. *Proc. Roy. Soc. London* **A363**, 525-546.
- Alber, I.E., and P.G. Saffman, 1978: Stability of Random Nonlinear Deepwater Waves with Finite Bandwidth Spectra. 31326-6035-RU-), TRW Defense and Space System Group.
- Benjamin, T.B., and J.E. Feir, 1967: The desintegration of wavetrains on deep water. Part 1. Theory. *J. Fluid Mech.* **27**, 417-430.
- Benney, D., and A.C. Newell, 1967: The propagation of nonlinear wave envelopes. *J. Math. Phys.* **46**, 133-139.
- Caponi, E.A., P.G. Saffman, and H.C. Yuen, 1982: Instability and confined chaos in a nonlinear dispersive wave system. *Phys. Fluids* **25**, 2159-2166.
- Cohen, B.I., K.M. Watson, and B.J. West, 1976: Some properties of deep water solitons. *Phys. Fluids* **19**, 345-350.
- Crawford, D.R., P.G. Saffman, and H.C. Yuen, 1980: Evolution of a Random Inhomogeneous Field of Nonlinear-Deep-Water Gravity Waves. *Wave Motion* **2**, 1-16.
- Crawford, D.R., B.M. Lake, P.G. Saffman, and H.C. Yuen, 1981: Stability of weakly nonlinear deep-water waves in two and three dimensions. *J. Fluid Mech.* **105**, 177-191.
- Davidson, R.C., 1972: *Methods in nonlinear plasma theory*. Academic Press, New York and London, 356p.
- Davey, A., 1972: The propagation of a weak nonlinear wave. *J. Fluid Mech.*, **53**, 769-781.
- Dean, R.G., 1990: Freak waves: A possible explanation. In A. Torum & O.T. Gudmestad (Eds.), *Water Wave Kinematics* (pp. 609-612), Kluwer.
- Draper, L., 1965: 'Freak' ocean waves. *Marine Observer* **35**, 193-195.
- Dysthe, K.B., 1979: Note on a modification to the nonlinear Schrödinger equation for application to deep water waves. *Proc. Roy. Soc. London* **A369**, 105-114.
- Hasimoto, H., and H. Ono, 1972: Nonlinear modulation of gravity waves. *J. Phys. Soc. Japan*, **33**, 805-811.
- Hasselmann, K., 1962: On the non-linear energy transfer in a gravity-wave spectrum, part 1: general theory. *J. Fluid Mech.* **12**, 481.
- Hasselmann, K., T.P. Barnett, E. Bouws, H. Carlson, D.E. Cartwright, K. Enke, J.A. Ewing, H. Gienapp, D.E. Hasselmann, P. Kruseman, A. Meerburg,

P. Müller, D.J. Olbers, K. Richter, W. Sell, and H. Walden, 1973: Measurements of wind-wave growth and swell decay during the Joint North Sea Wave Project (JONSWAP), *Dtsch. Hydrogr. Z. Suppl. A* **8(12)**, 95p.

Janssen, P.A.E.M., 1983a: On a fourth-order envelope equation for deep-water waves. *J. Fluid Mech.* **126**, 1-11.

Janssen, P.A.E.M., 1983b: Long-time behaviour of a Random Inhomogeneous Field of Weakly Nonlinear Surface Gravity Waves. *J. Fluid Mech.* **133**, 113-132.

Janssen, P.A.E.M., 1991: On nonlinear wave groups and consequences for spectral evolution, pp 46-52 in *Directional ocean wave spectra* R.C. Beal (ed). The Johns Hopkins University Press, Baltimore, 218 p.

Janssen, P.A.E.M., and G.J. Komen, 1982: Modification of the Surface Elevation Probability Distribution in Ocean Swell by Nonlinear Spectral Broadening. *J. Geophys. Res.* **87**, 4155-4162.

Komen, G.J., L. Cavaleri, M. Donelan, K. Hasselmann, S. Hasselmann, and P.A.E.M. Janssen, 1994: *Dynamics and Modelling of Ocean waves*(Cambridge University Press, Cambridge)

Krasitskii, V.P., 1990: Canonical transformation in a theory of weakly nonlinear waves with a nondecay dispersion law. *Sov. Phys. JETP* **71**, 921-927.

Krasitskii, V.P., and V.A. Kalmykov, 1993: Four-wave Reduced Equations for Surface Gravity Waves. *Izvestiya, Atmospheric and Physics* **29**, 222-228.

Lake B.M., H.C Yuen, H. Rungaldier, and W.E. Ferguson, 1977: Nonlinear deep-water waves: Theory and experiment. Part 2. Evolution of a continuous wave train, *J. Fluid Mech.* **83**, 49-74.

Lavrenov, I., 1998: The wave energy concentration at the Agulhas current of South Africa. *Nat. Hazards* **17**,117.

Longuet-Higgins, M.S., 1978: The instabilities of gravity waves of finite amplitude in deep-water. II. Subharmonics. *Proc. Roy. Soc. London* **A360**, 489-505.

Martin, D.U., and H.C. Yuen, 1980: Quasi-recurring energy leakage in the two-space-dimensional nonlinear Schrödinger equation. *Phys. Fluids* **23**, 881-883.

Onorato, M., A.R. Osborne, M. Serio, and T. Damiani, 2000: Occurrence of Freak Waves from Envelope Equations in Random Ocean Wave Simulations, in *Proceedings of Rogue Waves 2000* (Ifremer, Brest 29,30 november 2000), eds. M. Olagnon and G.A. Athanassoulis

Osborne, A.R., M. Onorato, and M. Serio, 2000: The nonlinear dynamics of rogue waves and holes in deep water gravity wave trains. *Phys. Lett. A* **275**, 386-393.

Stokes, G.G., 1847: On the Theory of Oscillatory Waves. *Math. Phys. Pap.* **1**, 197-229.

Tanaka, M., 1992: The role of Modulational Instability. In the formation of Wave Groups, in M.L. Banner and R.H.J. Grimshaw(Eds.), *Breaking waves*(pp 237-242), Springer Verlag.

Trulsen K., and K. Dysthe, 1997: Freak Waves-A Three-dimensional Wave Simulation. in *Proceedings of the 21st Symposium on naval Hydrodynamics*(National Academy Press), pp 550-558.

Wigner, E., 1932: On the quantum correction for thermodynamic equilibrium. *Phys. Rev.* **40**, 749-759.

Wolfram J., and B. Linfoot, 2000: Some experiences in estimating long and short term statistics for extreme waves in the North Sea. Abstract for the *Rogue waves 2000 workshop*, Ifremer, Brest.

Yuen, H.C., and W.E. Ferguson, 1978: Relationship between Benjamin-Feir Instability and recurrence in the nonlinear Schrödinger equation. *Phys. Fluids* **21**, 1275-1278.

Yuen, H.C., and B.M. Lake, 1982: Nonlinear dynamics of deep water gravity waves. *Adv. Appl. Mech.* **22**, 67-229.

Zakharov, V.E., 1968: Stability of periodic waves of finite amplitude on the surface of a deep fluid. *J. Appl. Mech. Techn. Phys.* **9**, 190-194.

Zakharov, V.E., and N.N. Filonenko, 1968: The energy spectrum for random surface waves. *Dokl. Acad. Sci. USSR* **170**, 1291-1295.

Zakharov, V.E., and A.B. Shabat, 1972: Exact theory of two-dimensional self-focussing and one-dimensional self-modulating waves in nonlinear media. *Sov. Phys.-JETP (Engl. Transl.)* **34**, 62.

Zakharov, V.E., and A.M. Rubenchik, 1974: Instability of waveguides and solitons in nonlinear media. *Sov. Phys.-JETP (Engl. Transl.)* **38**, 494.

7. Figure captions

Fig. 1 Detail of surface elevation η as function of dimensionless time t' . The top panel a) shows the time series for a fixed choice of initial phase, $\theta = 0$, while the bottom panel b) shows the time series for a random choice of initial phase.

Fig. 2 The surface elevation probability distribution as function of normalized height, $\eta/\sqrt{m_0}$ (with m_0 the variance), corresponding to the cases of Fig. 1. For reference the Gaussian distribution is shown as well.

Fig. 3 Time evolution of spectral width for several values of the BF Index. Corresponding results from homogeneous theory are shown as well.

Fig. 4 Initial and final time wave number spectrum according to the Monte Carlo Forecasting of Waves (MCFW) using the nonlinear Schrödinger Equation. Error bars give 95% confidence limits. Results from theory are shown as well.

Fig. 5 Relative spectral broadening $(\sigma_k(t'_\infty) - \sigma_k(0))/\sigma_k(0)$ as function of the BF Index. Shown are results for focussing (BF) and defocussing (no BF) from the simulations and from theory, but results from theory are identical for these two cases.

Fig. 6 Final time versus initial time value of the BF Index for the same cases as displayed in Fig.5.

Fig. 7 Probability distribution function for surface elevation as function of normalized height $\eta/\sqrt{m_0}$. Results from numerical simulations with the nonlinear Schrödinger equation and homogeneous theory in case of focussing (BF Index of 1.4). For reference the Gaussian distribution is shown as well. To emphasize the extremes the logarithm of the pdf has been plotted. Freak waves correspond to a normalized height of 4.4 or larger, hence nonlinearity has a dramatic impact on the occurrence of freak waves.

Fig. 8 Normalized Kurtosis as function of the BF Index. Shown are results for focussing (BF) and defocussing (no BF) from the simulations and from theory. The theoretical result for defocussing can be obtained from the results of focussing by a reflection with respect to the x -axis.

Fig. 9 Probability distribution function for surface elevation as function of normalized height $\eta/\sqrt{m_0}$. Results from numerical simulations with the nonlinear Schrödinger equation and homogeneous theory in case of defocussing (BF Index of 1.4). For reference the Gaussian distribution is shown as well.

Fig. 10 Initial and final time wave number spectrum according to Monte Carlo Forecasting of Waves (MCFW) using the Zakharov equation. Error bars give 95% confidence limits. Results from theory are shown as well.

Fig. 11 Comparison of curves of final time versus initial value of the BF Index from simulations with the nonlinear Schrödinger equation and from the Zakharov equation. The corresponding theoretical results are shown as well.

Fig. 12 Normalized Kurtosis as function of the BF Index. Shown are results for focussing from simulations with the nonlinear Schrödinger equation and with the Zakharov equation. The corresponding theoretical results are shown as well.

Fig. 13 Final time peak wave number down-shift versus BF Index. Shown is a comparison between numerical simulation results from the Zakharov equation and theory.

Fig. 14 Time evolution of a measure for inhomogeneity, I , for two different ensemble sizes, according to the nonlinear Schrödinger equation.

Fig. 15 Time evolution of Hamiltonian E of the nonlinear Schrödinger equation. Also shown are time evolution of E according to lowest order inhomogeneous theory (E_{approx}) and according to homogeneous theory that includes the fourth cumulant. Finally, shown are the nonlinear contribution to E for a strictly Gaussian state (NL(C4=0)), and including all higher order cumulants (NL+C4).

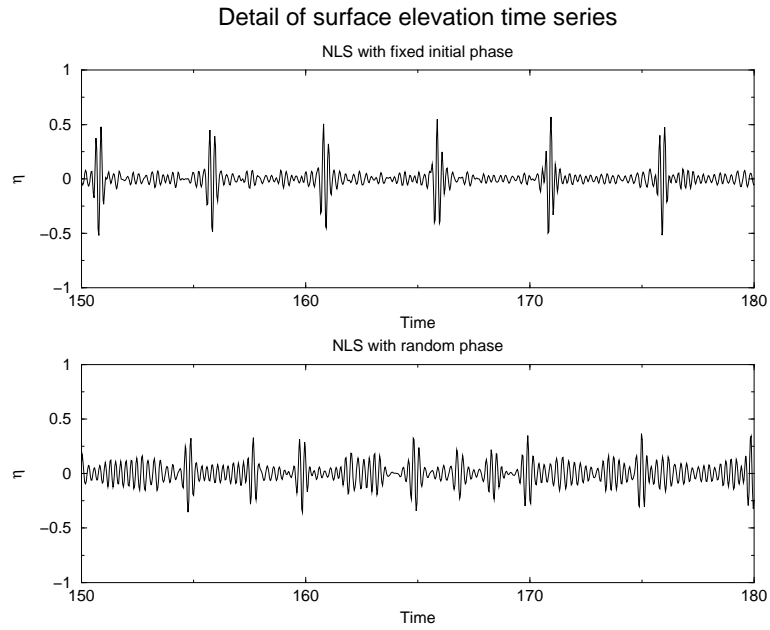


Fig. 1. Detail of surface elevation η as function of dimensionless time t' . The top panel a) shows the time series for a fixed choice of initial phase, $\theta = 0$, while the bottom panel b) shows the time series for a random choice of initial phase.

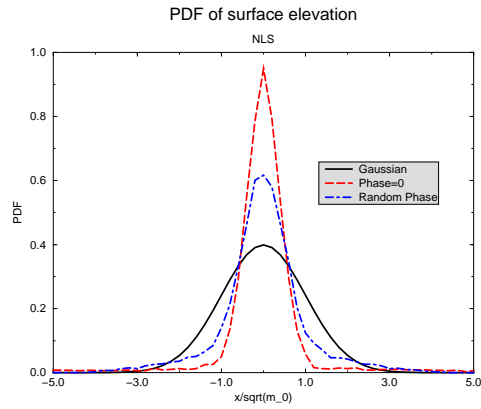


Fig. 2. The surface elevation probability distribution as function of normalized height, $\eta/\sqrt{m_0}$ (with m_0 the variance), corresponding to the cases of Fig. 1. For reference the Gaussian distribution is shown as well.

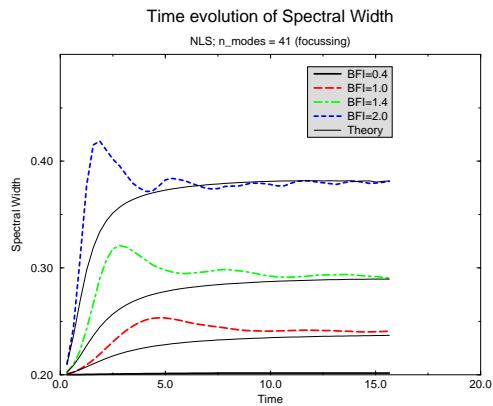


Fig. 3. Time evolution of spectral width for several values of the BF Index. Corresponding results from homogeneous theory are shown as well.

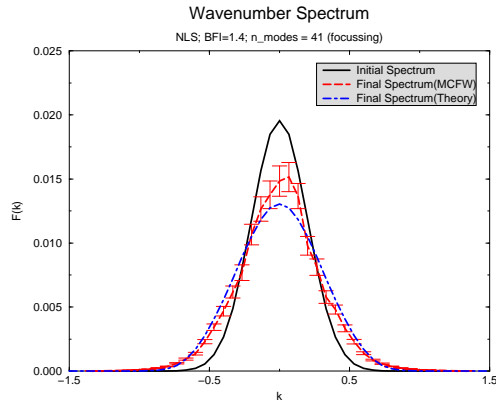


Fig. 4. Initial and final time wave number spectrum according to the Monte Carlo Forecasting of Waves (MCFW) using the nonlinear Schrödinger Equation. Error bars give 95% confidence limits. Results from theory are shown as well.

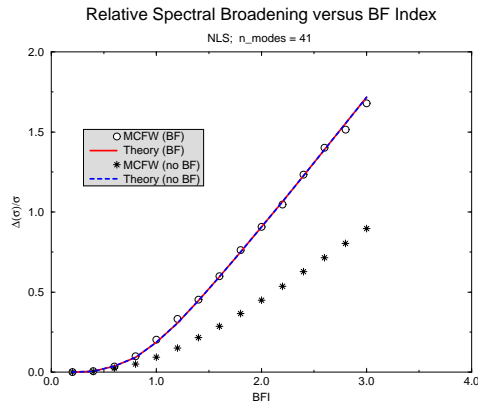


Fig. 5. Relative spectral broadening $(\sigma_k(t'_\infty) - \sigma_k(0))/\sigma_k(0)$ as function of the BF Index. Shown are results for focussing (BF) and defocussing (no BF) from the simulations and from theory, but results from theory are identical for these two cases.

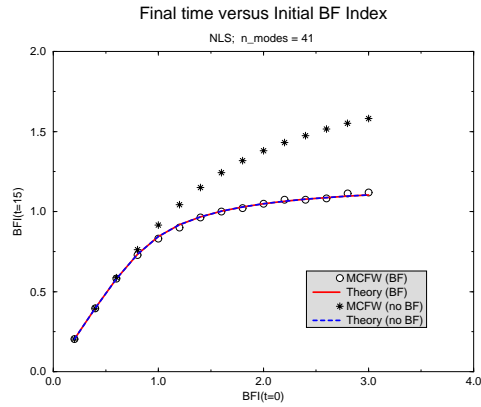


Fig. 6. Final time versus initial time value of the BF Index for the same cases as displayed in Fig.5.

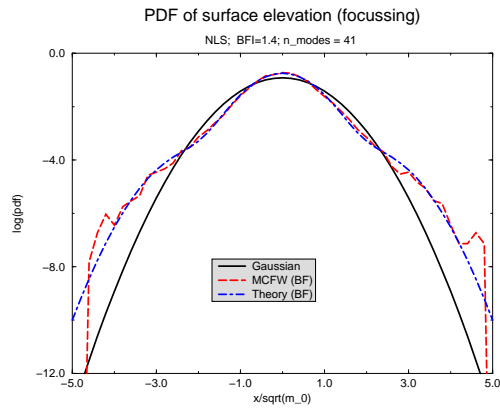


Fig. 7. Probability distribution function for surface elevation as function of normalized height $\eta/\sqrt{m_0}$. Results from numerical simulations with the nonlinear Schrödinger equation and homogeneous theory in case of focussing (BF Index of 1.4). For reference the Gaussian distribution is shown as well. Freak waves correspond to a normalized height of 4.4 or larger.

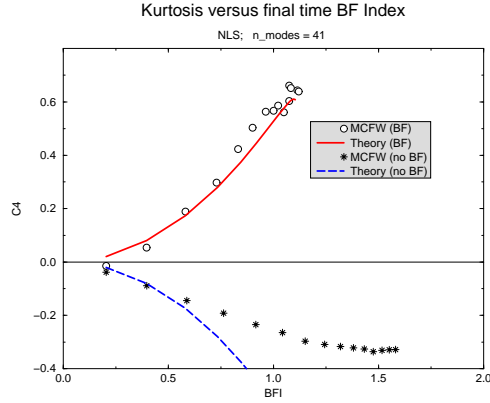


Fig. 8. Normalized Kurtosis as function of the BF Index. Shown are results for focussing (BF) and defocussing (no BF) from the simulations and from theory. The theoretical result for defocussing can be obtained from the results of focussing by a reflection with respect to the x -axis.

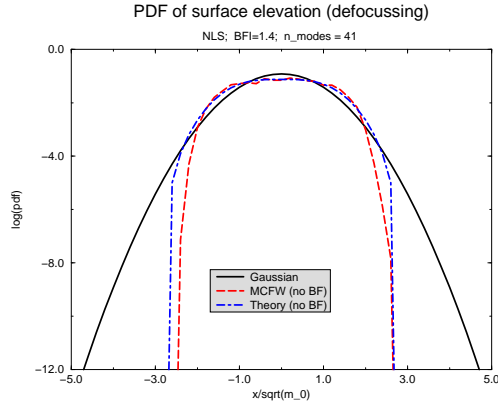


Fig. 9. Probability distribution function for surface elevation as function of normalized height $\eta/\sqrt{m_0}$. Results from numerical simulations with the nonlinear Schrödinger equation and homogeneous theory in case of defocussing (BF Index of 1.4). For reference the Gaussian distribution is shown as well.

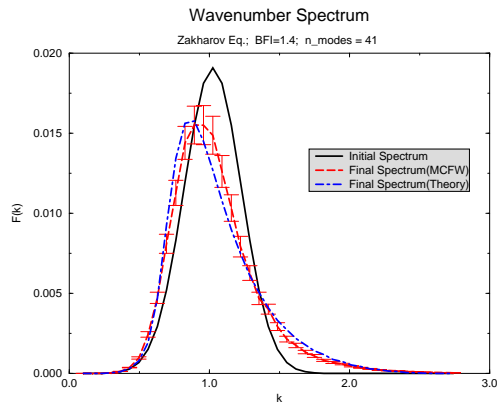


Fig. 10. Initial and final time wave number spectrum according to Monte Carlo Forecasting of Waves (MCFW) using the Zakharov equation. Error bars give 95% confidence limits. Results from theory are shown as well.

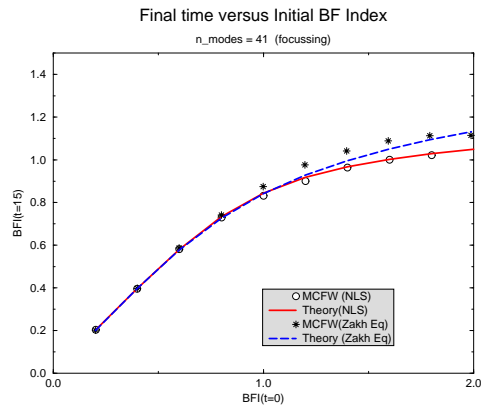


Fig. 11. Comparison of curves of final time versus initial value of the BF Index from simulations with the nonlinear Schrödinger equation and from the Zakharov equation. The corresponding theoretical results are shown as well.

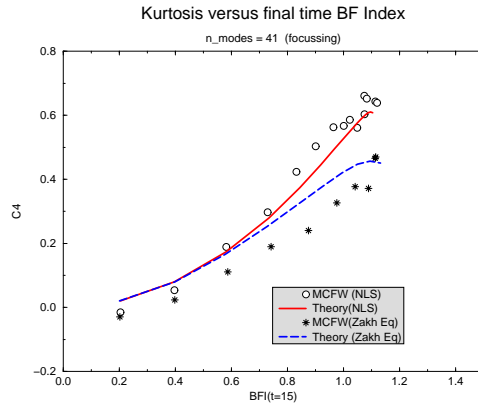


Fig. 12. Normalized Kurtosis as function of the BF Index. Shown are results for focussing from simulations with the nonlinear Schrödinger equation and with the Zakharov equation. The corresponding theoretical results are shown as well.

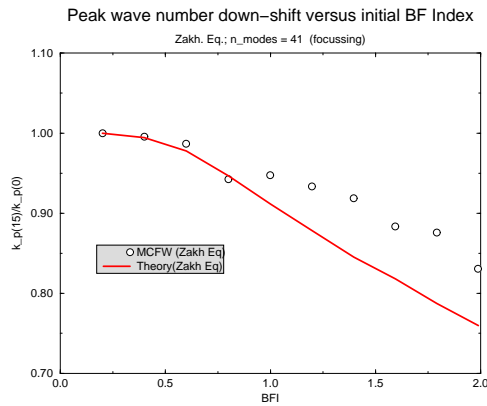


Fig. 13. Final time peak wave number down-shift versus BF Index. Shown is a comparison between numerical simulation results from the Zakharov equation and theory.

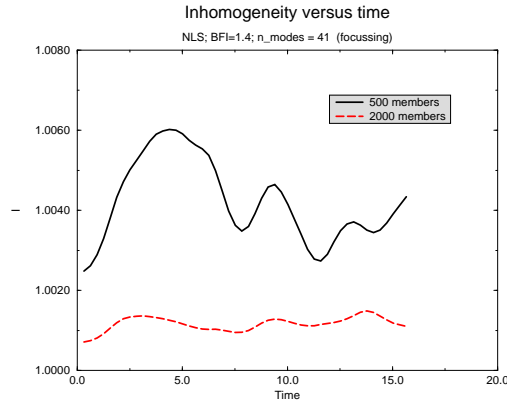


Fig. 14. Time evolution of a measure for inhomogeneity, I , for two different ensemble sizes, according to the nonlinear Schrödinger equation.

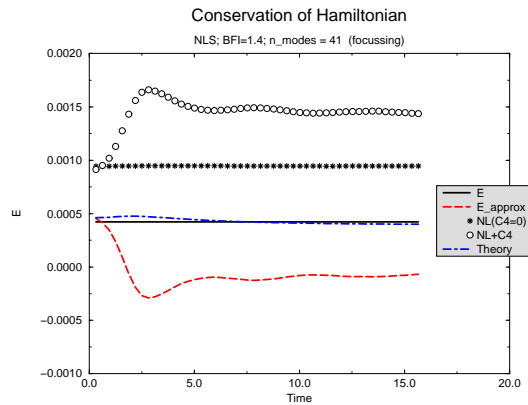


Fig. 15. Time evolution of Hamiltonian E of the nonlinear Schrödinger equation. Also shown are time evolution of E according to lowest order inhomogeneous theory (E_{approx}) and according to homogeneous theory that includes the fourth cumulant. Finally, shown are the nonlinear contribution to E for a strictly Gaussian state ($NL(C4=0)$), and including all higher order cumulants ($NL+C4$).